IEEE Access
Multidisciplinary | Rapid Review | Open Access Journal

Received May 8, 2018, accepted June 8, 2018, date of publication June 25, 2018, date of current version September 5, 2018.

Digital Object Identifier 10.1109/ACCESS.2018.2849599

A Modified Moth Swarm Algorithm Based on an Arithmetic Crossover for Constrained Optimization and Optimal Power Flow Problems

SERHAT DUMAN, (Member, IEEE)
Department of Electrical and Electronics Engineering, Technology Faculty, Duzce University, 81620 Duzce, Turkey
e-mail: serhatduman@duzce.edu.tr

ABSTRACT The moth swarm algorithm (MSA) is a new meta-heuristic optimization technique inspired by the navigational style of moths in nature. This paper represents a novel modified MSA with an arithmetic crossover (MSA-AC) with the aim of improving the search for a global optimum, the convergence speed to an optimal solution, and the performance of the traditional MSA. The proposed MSA-AC method was applied in 23 standard benchmark test functions and used in six CEC 2005 composite benchmark test functions. Furthermore, in order to verify the success of the optimal solution, the MSA-AC approach was used to solve the optimal power flow problem in the two-terminal high-voltage direct current systems of the modified New England 39-bus and the modified WSCC 9-bus test systems. The numerical results obtained from the MSA-AC were compared with both the traditional MSA method and with various optimization algorithms presented in the literature. The outcomes obtained from the comparative results indicate the potential of the proposed approach in finding the global optimum and the convergence to an optimal solution.

INDEX TERMS Moth swarm algorithm, arithmetic crossover, benchmark test functions, optimal power flow, HVDC.

I. INTRODUCTION

To date, the classical mathematical optimization approaches remain incapable of solving difficult high-dimensional problems. Thus, stochastic optimization approaches based on population have been enhanced to solve these types of optimization problems. The well-known optimization algorithms include the Differential Evolutionary Algorithm (DE) [1], Harmony Search Algorithm (HSA) [2], Black Hole (BH) [3], Ray Optimization (RO) [4], Genetic Algorithm [5], Big-Bang Big-Crunch (BBBC) [6], Firefly Algorithm (FA) [7], Krill Herd (KH) [8], Teaching Learning Based Optimization (TLBO) [9], Vortex Search Algorithm (VSA) [10], Salp Swarm Algorithm (SSA) [11], Whale Optimization Algorithm (WOA) [12], Sine Cosine Algorithm (SCA) [13], Tree Seed Algorithm (TSA) [14], Dragonfly Algorithm (DA) [15], Grey Wolf Optimizer (GWO) [16], Multi-Verse Optimizer [17] and Moth Swarm Algorithm (MSA) [18]. In the literature, the meta-heuristic optimization approaches have been overused by researchers. This includes not only use of the benchmark test functions of the optimization field but also use of real-world optimization problems in scientific fields. The main purpose of the stochastic techniques is to provide a means to reach the best solution, whether for benchmark optimization or realistic optimization problems. In order to reach the best solution, these algorithms should be dominated by two fundamental features: exploration and exploitation. Exploration is defined as the ability of the algorithm to provide for a diversity of solutions and for the changing of created candidate solutions in order to find the best solution value in the search space for the optimization problem. Exploitation is expressed as doing a local search by narrowing the scope of the candidate solutions around the obtained good solutions. This way provides for the improvement of solution quality and the convergence ability of the algorithm to achieve the best outcome [12], [13], [19], [20]. Consequently, the balance between the features of exploration and exploitation of the stochastic optimization algorithms are very important to the solution of optimization problems.

Many optimization problems exist in the operation and planning of modern power systems. These problems can

2169-3536 © 2018 IEEE. Translations and content mining are permitted for academic research only.
Personal use is also permitted, but republication/redistribution requires IEEE permission.
See http://www.ieee.org/publications_standards/publications/rights/index.html for more information.

be listed as economic dispatch, combined economic dispatch, dynamic economic dispatch, scheduling of short-term hydrothermal generation, combined heat and power dispatch, optimal power flow, optimal power flow with flexible alternating current transmission system (FACTS) devices, optimal AC-DC power flow, optimal reactive power flow, load frequency control, etc. In recent years, the global energy demand has steadily risen due to the increasing population and the developments in technology. In order to meet this energy demand, either new generating units or new alternating current transmission lines and high-voltage direct current (HVDC) links are required [21]. In addition, due to the increasing energy demand, the planning and operation of the power systems under optimal conditions have become increasingly important. Thus, the optimal power flow (OPF) problem is one of the most significant problems in the operation and planning of modern power systems. The main goal is to satisfy both equality and inequality by minimizing the total fuel cost of the generating units. Furthermore, many heuristic approaches for solving the OPF problem have been presented in the literature [22]–[30]. Nowadays, the research on power system planning has concentrated on power transfer through HVDC links. The HVDC systems can provide many advantages related to power system application. For instance, reactive power is not transferred by these systems and the energy loss is less compared to AC transmission systems; thus, these systems are used to stabilize power systems [31]. Recently, researchers have been using heuristic methods to handle the OPF problem of HVDC systems [32]–[37].

The moth swarm algorithm (MSA) is a stochastic algorithm inspired by the navigational style of moths in nature. This algorithm was introduced by Ali Mohamed et al. (2017), who used it to solve the OPF problem. According to their simulation results, the MSA provided a better way of finding a solution than the other stochastic techniques [18]. The current paper presents a new version, the MSA-AC method, based on the population diversity of the MSA method combined with an arithmetic crossover (AC) operator. This MSA-AC has been proposed in order to improve the applicability, the convergence velocity to the optimal solution, the performance and the efficiency of the traditional MSA approach. In addition, the selected pathfinder moths in reconnaissance phase were updated by using an AC operator to increase the exploration and exploitation features of the algorithm. The proposed MSA-AC approach was tested to find the global optimal solution in 23 standard benchmark test functions and six of the composite benchmark test functions presented in the CEC 2005 special session and to solve the OPF problem of two-terminal HVDC systems.

The remainder of the paper is structured as follows. The MSA approach and the proposed MSA-AC approach are presented in Section 2. Section 3 presents the experimental results obtained from both the benchmark test functions and the OPF problem of two-terminal HVDC systems. Section 4 presents the conclusions of this study.

II. THE PROPOSED MOTH SWARM ALGORITHM WITH ARITHMETIC CROSSOVER

A. MOTH SWARM ALGORITHM

The MSA was first proposed by Ali Mohamed et al., who were inspired by the simulation of the behavior of moths in nature. The position of the light source in MSA is expressed as the search space for potential solutions to optimization problems. The brightness of this light source was considered by the authors as the fitness of the potential solution. In order to model the MSA approach, the moths are considered as three groups: pathfinders, prospectors and onlookers [18].

In the pathfinder group, the authors proposed using a small group in the population to find new areas in the search space for the solution of optimization problems. By finding the best position of the light source, this group leads other members in the population to this position. The moths in the second group, the prospectors, try to drift in a random spiral path around the light source that has been marked by the pathfinders. Finally, the onlookers of the third group move towards the best optimal solution obtained by the prospectors. The MSA is expressed in four main phases: initialization, reconnaissance, transverse orientation and celestial navigation [18].

1) INITIALIZATION

In the initialization phase, the search space with the d-dimension and n-number of the population is generated within values of the specified limit for the solution of the optimization problem. The initial candidate solutions created in the search space of the algorithm are mathematically explained as follows [18]:

$$x_{ij} = rand\,[0,\,1] \times \left(x_j^{\max} - x_j^{\min}\right) + x_j^{\min} \quad \begin{matrix} i = 1, 2, \ldots, n \\ j = 1, 2, \ldots, d \end{matrix} \tag{1}$$

The rand [0, 1] is a random number between zero and one. After the creation of the candidate solutions, the fitness function is computed for the candidate moths in the population. The group of each moth is identified according to the fitness values. Thus, the moths comprising the best solutions are selected as the pathfinders and the moths consisting of the next best and worse solutions are selected as the prospectors and onlookers, respectively [18].

2) RECONNAISSANCE PHASE

In this phase, the updating of the positions of the pathfinders is carried out in five steps. The first step is using the diversity index for the crossover points. The normalized dispersal degree at t∼iteration is calculated as follows:

$$\sigma_j^t = \frac{\sqrt{\frac{1}{n_p}\sum_{i=1}^{n_p}\left(x_{ij}^t - \overline{x_j^t}\right)^2}}{\overline{x_j^t}} \tag{2}$$

Where the number of pathfinder moths is named as n_p.

$\overline{x_j^t}$ and the variation coefficients μ^t are defined as follows:

$$\overline{x_j^t} = \frac{1}{n_p}\sum_{i=1}^{n_p} x_{ij}^t \tag{3}$$

$$\mu^t = \frac{1}{d}\sum_{j=1}^{d} \sigma_j^t \tag{4}$$

In the second step, the random processes based on α-stable distribution are explained as Lévy flights. In the third step, the sub-trial vectors $\left(\overrightarrow{v_p}\right)$ are created by using host vectors $\left(\overrightarrow{x_p}\right)$ and donor vectors $\left(\overrightarrow{x_{r1}}\right)$ in the mutation operator as the difference vectors Lévy mutation.

In the fourth step, the position of each pathfinder is updated by using the adaptive crossover operation based on population diversity. In the final step, the selection strategy is implemented to determine the fitter solutions at the next iteration. For further details about the reconnaissance phase procedures of the MSA, readers can benefit by examining reference [18].

3) TRANSVERSE ORIENTATION

The prospectors are defined as the group of moths having the next level of luminescence intensities and n_f represents the number of prospectors that reduce dependence on the iteration. This can be mathematically explained as follows [18]:

$$n_f = round\left(\left(n - n_p\right) \times \left(1 - \frac{t}{T}\right)\right) \tag{5}$$

The T is number of the maximum iteration. The position of each prospector (x_i) is updated for the next iteration by using formula (6) with respect to the spiral flight path.

$$x_i^{t+1} = |x_i^t - x_p^t| \times e^{\theta} \times \cos 2\pi\theta + x_p^t \quad \forall p \in \{1, 2, \ldots, n_p\}, \; i \in \left\{n_p + 1, n_p + 2, \ldots, n_f\right\} \tag{6}$$

Where $\theta \in [r, 1]$ is a random number and $r = -1 - t/T$.

Due to each moth constantly changing groups, greater luminescence can be found than with the existing light sources by any prospector moth encouraged to become a pathfinder moth [18].

4) CELESTIAL NAVIGATON

During the iteration process in the algorithm, the number of prospectors in the search space is reduced, while the number of onlookers increases. The onlooker moths have the lowest luminescent sources. Hence, the moths of this group try to move towards the shiniest solution. The onlookers were investigated as two components: *gaussian walks* and *associative learning mechanism with immediate memory*, respectively. The encouraging areas in the search space were examined in the Gaussian walks. According to Gaussian walks, the new onlooker moths for the next iteration are defined as follows [18]:

$$x_i^{t+1} = x_i^t + \varepsilon_1 + \left[\varepsilon_2 \times best_g^t - \varepsilon_3 \times x_i^t\right] \quad \forall i \in \{1, 2, \ldots, n_G\} \tag{7}$$

$$\varepsilon_1 \sim random\,(size\,(d)) \oplus N\left(best_g^t, \frac{\log t}{t} \times \left(x_i^t - best_g^t\right)\right) \tag{8}$$

where ε_1 are random samples which are handled from gaussian stochastic distribution, $best_g$ is the global best solution and ε_2 and ε_3 are random numbers (0, 1). In the associative learning mechanism, the onlooker moths benefit from the associative learning abilities providing communication between moths. The new onlooker moths for the next generation can be mathematically expressed as follows [18]:

$$x_i^{t+1} = x_i^t + 0.001 \times G\left[x_i^t - x_i^{\min}, x_i^{\max} - x_i^t\right] + \left(1 - \frac{g}{G}\right) \times r_1 \times \left(best_p^t - x_i^t\right) + 2g/G \times r_2\left(best_g^t - x_i^t\right) \tag{9}$$

B. PROPOSED MOTH SWARM ALGORITHM WITH ARITHMETIC CROSSOVER

In this paper, the arithmetic crossover (AC) operator in the genetic algorithm (GA) is combined with the crossover operator based on population diversity. The crossover operator is one of the affecting factors in the search for the global solution of the GA. Some of the selected solutions in the crossover operator are combined to produce a better solution by using different crossover operators which provide for the reproduction of a new individual. In addition, this provides rapid convergence to the optimal solution of the GA. The AC operator is used by considering the advantage of the used crossover operators in the GA for the improvement of the MSA. The success in finding the global solution of the traditional MSA is increased by using the AC in the reconnaissance phase of the proposed MSA-AC. Before the crossover operator based on population diversity is used, two moths are selected from the pathfinders used in the reconnaissance phase in order to produce two new moths in the AC. These two new moths are produced by using the following equation [38]:

$$\begin{aligned} x_1 &= a \times x_i^1 + (1 - a) \times x_i^2 \quad a \in (0, 1) \\ x_2 &= (1 - a) \times x_i^1 + a \times x_i^2 \end{aligned} \tag{10}$$

where $\boldsymbol{a}$ is a random number between the interval (0, 1), $\boldsymbol{x_{1,2}}$ are the newly produced moths and $\boldsymbol{x_i^1}, \boldsymbol{x_i^2}$ are the selected moths. The fitness functions of the two newly produced moths are calculated. The selection strategy is then applied to determine the produced moth having the best fitness value according to the AC. In this way, the position of the new moth is determined in the next iteration. This strategy is

mathematically expressed as follows:

$$fit_i^{t+1} = \begin{cases} fit_i & if\ fit_1 \langle fit_2 \\ fit_i & if\ fit_2 \langle fit_1 \end{cases} \quad i \in (1, n_p)$$
$$x_i^{t+1} = \begin{cases} x_i & if\ x_1 \langle x_2 \\ x_i & if\ x_2 \langle x_1 \end{cases} \tag{11}$$

Here, $\boldsymbol{i}$ is a number between the interval (1,n_p), which is used to determine a grain pathfinder. After the position of the moth in the next iteration is indicated according to the AC, the positions of the other pathfinder moths are determined by using the crossover operator based on the population diversity for the next iteration. Figure 1 shows the flowchart of the proposed MSA-AC algorithm.

III. EXPERIMENTAL STUDIES

A. EXPERIMENTAL STUDY 1: APPLICATION OF THE MSA-AC TO BENCHMARK FUNCTIONS

In order to evaluate the efficiency, the robustness and the performance of the proposed MSA-AC algorithm, it was tested in 23 standard benchmark test functions and six composite benchmark test functions conceived in the CEC 2005 special session. These standard benchmark and composite benchmark test functions were taken from references [39]–[41].

Tables 1-3 and Table 4 show the benchmark test functions and composite benchmark test functions, respectively. For verification of the obtained results of the proposed MSA-AC, the well-known TLBO, FA, MVO, SSA and DA optimization algorithms are chosen. The number of populations and the number of maximum iterations for the MSA-AC and the used other optimization algorithms were selected as 30 populations, 1000 iterations for the f_1-f_9 test functions and 500 iterations for the f_{10}-f_{29} test functions, respectively.

The results of the MSA-AC and the other algorithms for the unimodal test functions are presented in Table 5. These algorithms were run 30 times for all test functions. The convergence curves of the proposed MSA-AC, the classical MSA, TLBO, FA, SSA, DA and MVO algorithms for the chosen unimodal test functions are shown in Figure 2. Table 5 reveals that the proposed MSA-AC method achieved better results than the classical MSA and the other optimization algorithms in the literature. However, the maximum and standard deviation values of the TLBO for the f_5 function and the maximum values obtained with the MSA method for the f_6 function were better than those results of the MSA-AC method.

The multimodal test functions indicated in Table 2 have many local minima. In addition, these functions are depicted as difficult problems within the optimization problem. The results obtained from the proposed MSA-AC and the other MSA, TLBO, FA, SSA, DA and MVO algorithms for the multimodal test functions are shown in Table 6. These algorithms were run 30 times for the multimodal test functions. Figure 3 shows the convergence curves of the MSA-AC and the used optimization algorithms. It can be seen in Table 6 that the proposed MSA-AC method achieved better result than the MSA approach. However, no difference was seen in the results of the MSA method and those of the proposed MSA-AC method for the f_9, f_{10} and f_{11} test functions. Additionally, the obtained results from the FA for the f_{13} function were better than those obtained results from the proposed approach.

The f_{14} to f_{23} benchmark test functions are defined as multimodal low-dimensional benchmark test functions, and are presented in Table 3. The comparison results of the proposed MSA-AC approach and the used optimization algorithms are given in Table 7. It is quite apparent from all the analyzation results (best, mean, max., std., etc.) that the proposed MSA-AC method achieved better results for these test functions than the MSA and the other optimization methods. However, the obtained all values of the TLBO for the f_{14} and the maximum value of the TLBO for the f_{15} functions, the standard deviation value obtained with the SSA method for the f_{15} function and the maximum value of the FA for the f_{20} function were better than the results of proposed MSA-AC method.

The composite test functions were used to better reflect that real-world problems are generally more challenging compared to multimodal test functions. In order to find the global solution value of the test functions in this type of structure, the optimization algorithms used ought to display an adequate balance between exploitation and exploration. Thus, it can be seen that the proposed MSA-AC approach was able to balance exploration and exploitation for the solution of these type of problems. The results of the proposed MSA-AC approach and the used other optimization approaches for the composite test functions are presented in Table 8. These algorithms were run 30 times for the composite test functions. The results revealed that the proposed MSA-AC algorithm provided more competitive solutions for the composite benchmark test functions compared with the used optimization methods. Figure 4 shows the convergence curves of the MSA-AC and the other algorithms. It is clear from the figure that the MSA-AC approach was more efficient in convergence to the optimal solution compared to the used optimization methods.

B. EXPERIMENTAL STUDY 2: APPLICATION OF THE MSA-AC TO THE OPF OF THE TWO-TERMINAL HVDC SYSTEMS

In modern power system planning, the OPF problem is defined as a nonlinear and non-convex optimization problem. The main goal is to minimize the total fuel cost of the generating units within the specified equality and inequality constraints. In this experimental study, the OPF problem was considered as that of two-terminal HVDC systems. The mathematical equation of the OPF problem is described as follows:

$$\text{Minimize } f(x, u) \tag{12}$$
$$\text{Subject to } g(x, u) = 0$$
$$h(x, u) \leq 0 \tag{13}$$

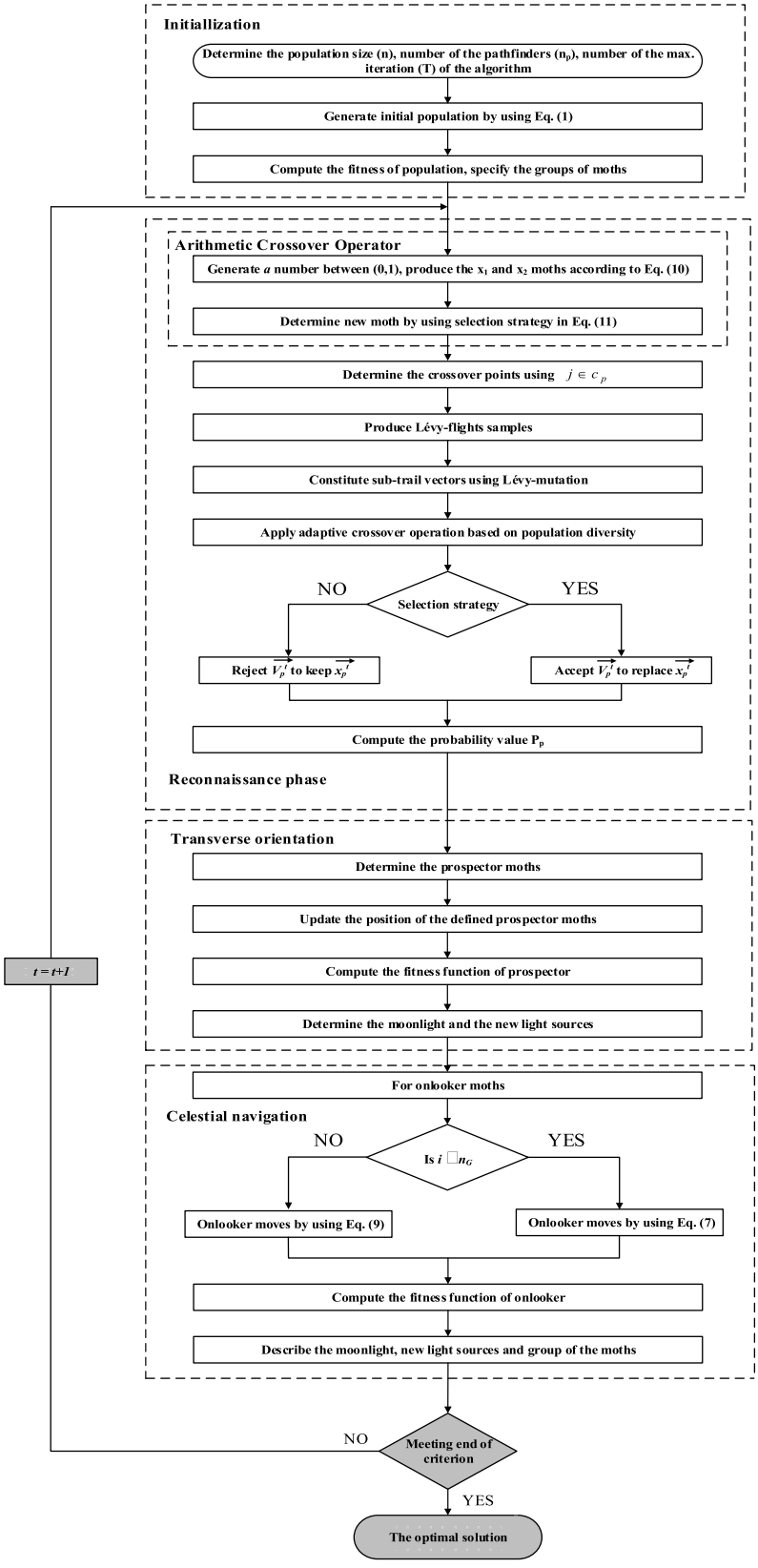

FIGURE 1. Flowchart of the proposed MSA-AC.

TABLE 1. Unimodal test functions.

Test function	Dim	Range
$f_1(x)=\sum_{i=1}^{n} x_i^2$	30	[-100,100]
$f_2(x)=\sum_{i=1}^{n}\lvert x_i\rvert+\prod_{i=1}^{n}\lvert x_i\rvert$	30	[-10,10]
$f_3(x)=\sum_{i=1}^{n}\left(\sum_{j=1}^{i} x_j\right)^2$	30	[-100,100]
$f_4(x)=\max_i\{\lvert x_i\rvert,1\le i\le n\}$	30	[-100,100]
$f_5(x)=\sum_{i=1}^{n-1}\left[100\left(x_{i+1}-x_i^2\right)^2+\left(x_i-1\right)^2\right]$	30	[-30,30]
$f_6(x)=\sum_{i=1}^{n}\left(\lfloor x_i+0.5\rfloor\right)^2$	30	[-100,100]
$f_7(x)=\sum_{i=1}^{n} ix_i^4+random[0,1)$	30	[-1.28,1.28]

TABLE 2. Multimodal test functions.

Test function	Dim	Range
$f_8(x)=\sum_{i=1}^{n}-x_i\sin\left(\sqrt{\lvert x_i\rvert}\right)$	30	[-500,500]
$f_9(x)=\sum_{i=1}^{n}\left[x_i^2-10\cos(2\pi x_i)+10\right]$	30	[-5.12,5.12]
$f_{10}(x)=-20\exp\left(-0.2\sqrt{\frac{1}{n}\sum_{i=1}^{n}x_i^2}\right)-\exp\left(\frac{1}{n}\sum_{i=1}^{n}\cos(2\pi x_i)\right)+20+e$	30	[-32,32]
$f_{11}(x)=\frac{1}{4000}\sum_{i=1}^{n}x_i^2-\prod_{i=1}^{n}\cos\left(\frac{x_i}{\sqrt{i}}\right)+1$	30	[-600,600]
$f_{12}(x)=\frac{\pi}{n}\left\{\begin{array}{l}10\sin(\pi y_1)+\sum_{i=1}^{n-1}(y_i-1)^2\left[1+10\sin^2(\pi y_{i+1})\right]\\+(y_n-1)^2\end{array}\right\}+\sum_{i=1}^{n}u(x_i,10,100,4)$ $y_i=1+\frac{x_i+1}{4}, u(x_i,a,k,m)=\begin{cases}k(x_i-a)^m & x_i>a\\0 & -a<x_i<a\\k(-x_i-a)^m & x_i<-a\end{cases}$	30	[-50,50]
$f_{13}(x)=0.1\left\{\begin{array}{l}\sin^2(3\pi x_i)+\sum_{i=1}^{n}(x_i-1)^2\left[1+\sin^2(3\pi x_i+1)\right]+\\(x_n-1)^2\left[1+\sin^2(2\pi x_n)\right]\end{array}\right\}+\sum_{i=1}^{n}u(x_i,5,100,4)$	30	[-50,50]

Where the objective function of this problem is depicted as the total production cost of the generators in the entire power system. The power flow equations and the security limits of the entire power system are considered as equality and inequality constraints, respectively. The state and control variable vectors are depicted as $\boldsymbol{x}$ and $\boldsymbol{u}$ vectors. In power system planning the determination of the variables of the $\boldsymbol{x}$ and $\boldsymbol{u}$ vectors is an indispensable part of solving the OPF problem. The $\boldsymbol{x}$ state variables vector of the AC and DC system is defined as follows [21], [32], [37]:

$$\begin{aligned} x &= [x_{AC}, x_{DC}] \\ x_{AC} &= \left[P_{G_{slack}}, Q_{G1}, \ldots, Q_{GNG}, V_{L1}, \ldots, V_{LNPQ}\right] \\ x_{DC} &= [t_r, t_i, \alpha, \gamma, v_{dr}, v_{di}] \end{aligned} \tag{14}$$

P_{Gslack}, Q_G, V_L, NG and NPQ can be defined as the active power output of the slack bus, the reactive power value of generating units, the voltage magnitudes of the load

TABLE 3. Multimodal test functions with fix dimension.

Test function	Dim	Range
$f_{14}(x)=\left(\frac{1}{500}\sum_{j=1}^{25}\frac{1}{j+\sum_{i=1}^{2}(x_i-a_{ij})^6}\right)^{-1}$	2	[-65.536,65.536]
$f_{15}(x)=\sum_{i=1}^{11}\left[a_i-\frac{x_1(b_i^2+b_ix_2)}{b_i^2+b_ix_3+x_4}\right]^2$	4	[-5,5]
$f_{16}(x)=4x_1^2-2.1x_1^4+\frac{1}{3}x_1^6+x_1x_2-4x_2^2+4x_2^4$	2	[-5,5]
$f_{17}(x)=\left(x_2-\frac{5.1}{4\pi^2}x_1^2+\frac{5}{\pi}x_1-6\right)^2+10\left(1-\frac{1}{8\pi}\right)\cos x_1+10$	2	[-5,10]× [0,15]
$f_{18}(x)=\left[1+(x_1+x_2+1)^2(19-14x_1+3x_1^2-14x_2+6x_1x_2+3x_2^2)\right]\times$ $\left[30+(2x_1-3x_2)^2\times(18-32x_1+12x_1^2+48x_2-36x_1x_2+27x_2^2)\right]$	2	[-2,2]
$f_{19}(x)=-\sum_{i=1}^{4}c_i\exp\left(-\sum_{j=1}^{3}a_{ij}(x_j-p_{ij})^2\right)$	3	[0,1]
$f_{20}(x)=-\sum_{i=1}^{4}c_i\exp\left(-\sum_{j=1}^{6}a_{ij}(x_j-p_{ij})^2\right)$	6	[0,1]
$f_{21}(x)=-\sum_{i=1}^{5}\left[(x-a_i)(x-a_i)^T+c_i\right]^{-1}$	4	[0,10]
$f_{22}(x)=-\sum_{i=1}^{7}\left[(x-a_i)(x-a_i)^T+c_i\right]^{-1}$	4	[0,10]
$f_{23}(x)=-\sum_{i=1}^{10}\left[(x-a_i)(x-a_i)^T+c_i\right]^{-1}$	4	[0,10]

busses, the number of the generating units and the number of PQ busses for the AC system, respectively. t_r and t_i are transformer tap ratio at rectifier and inverter sides, α and γ are described as the ignition delay and extinction advance angles, respectively. v_{dr} and v_{di} are depicted as DC link voltages of the rectifier and inverter terminals. $\boldsymbol{u}$ control variables vector of the AC and DC system is expressed as follows [21], [32], [37]:

$$\begin{aligned} u &= [u_{AC}, u_{DC}] \\ u_{AC} &= [P_{G2}, \ldots, P_{GNG}, V_{G1}, \ldots, V_{GNG}, T_1, \ldots, T_{NT}] \\ u_{DC} &= [p_r, p_i, q_r, q_i, i_d] \end{aligned} \tag{15}$$

Where P_G, V_G, T, NT, p_r, p_i, q_r, q_i and i_d are specified as active power output of the all generators on the system that except at the slack bus, the voltage value of the generators, transformer tap ratio value, the number of transformers, active power of the rectifier side, active power of the inverter side, reactive power of the rectifier side, reactive power of the inverter side and direct current, respectively. In this study, the DC transmission system was based on the widely acclaimed suppositions in the literature. These suppositions are covered in detail in [32] and [37]. A two-terminal AC-DC transmission system is shown in Figure 5 [21], [32], [37].

In Figure 5, v_r and v_i are the ac voltage values (rms) at the ith and jth busses, i_r and i_i are the currents at the ac sides of the rectifier and inverter, δ_r and δ_i are phase angles, ξ_r and ξ_i are ac current angles, DC link resistance is defined as the r_{dc}. The mathematical equations of the rectifier terminal can be described for two terminal AC-DC system as follow [21], [32], [37]:

$$\begin{aligned} v_{dor} &= kt_r v_r \Rightarrow k = \frac{3\sqrt{2}}{\pi} \\ v_{dr} &= v_{dor}\cos\alpha - r_{cr} i_d \Rightarrow r_{cr} = \frac{3x_{cr}}{\pi} \\ p_r &= v_{dr} i_d \\ \phi_r &= \cos^{-1}(v_{dr}/v_{dor}) \\ q_r &= \left|p_r \tan \boldsymbol{\phi}_r\right| \end{aligned} \tag{16}$$

Where v_{dor}, r_{cr} and $\boldsymbol{\phi}_r$ are expressed as the open circuit DC voltage value, the commutating resistance and the phase angle between the AC voltage and the current at the rectifier side, respectively. The mathematical expression of the inverter terminal can be defined for two terminal

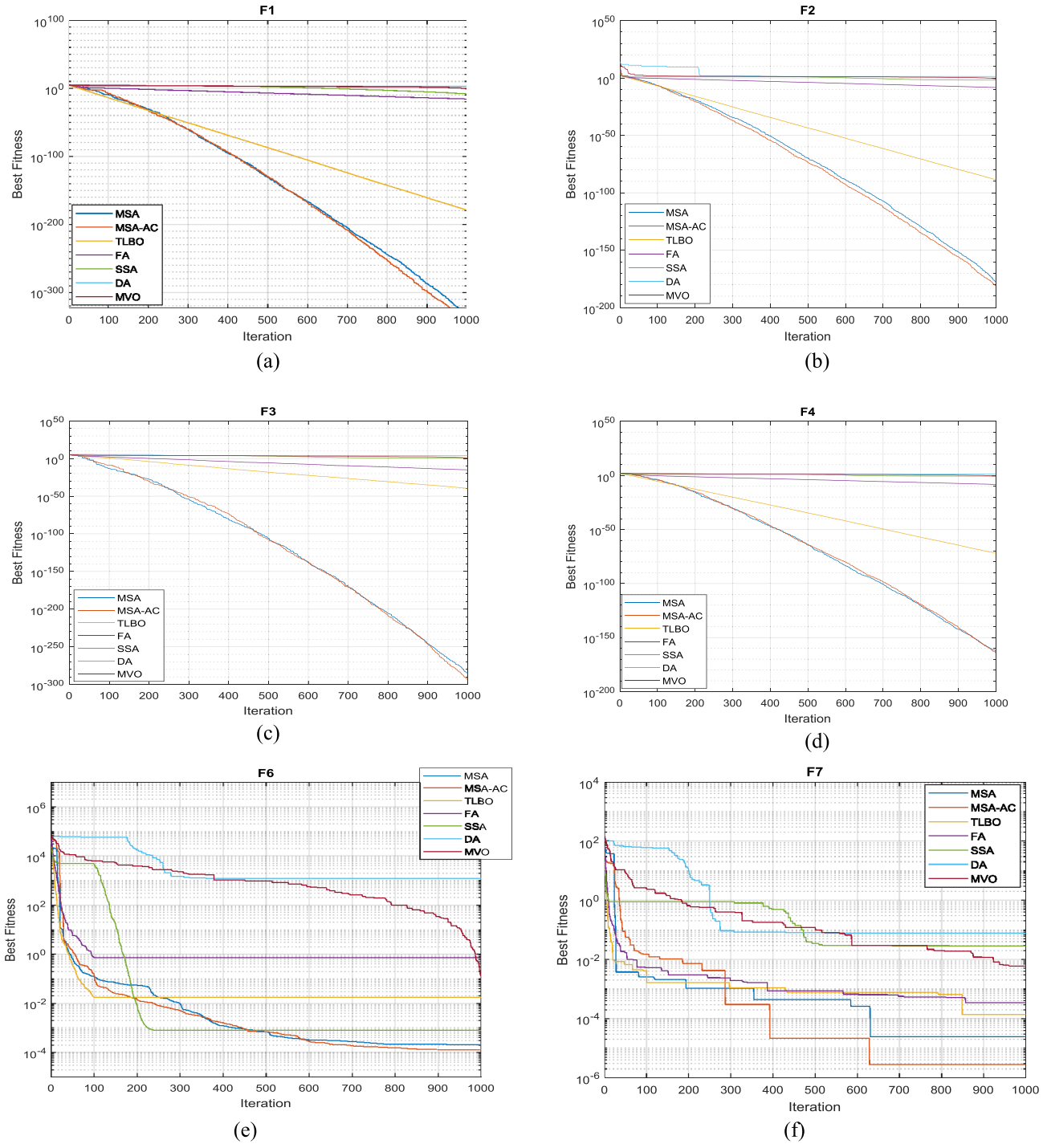

FIGURE 2. Convergence curves of the proposed MSA-AC and the other optimization algorithms for the unimodal test functions.

AC-DC system as follow [21], [32], [37]:

$$\begin{aligned} v_{doi} &= kt_i v_i \Rightarrow k = \frac{3\sqrt{2}}{\pi} \\ v_{di} &= v_{doi}\cos\gamma - r_{ci} i_d \Rightarrow r_{ci} = \frac{3x_{ci}}{\pi} \\ p_i &= v_{di} i_d \\ \phi_i &= \cos^{-1}\left(v_{di}/v_{doi}\right) \\ q_i &= |p_i \tan\phi_i| \end{aligned} \tag{17}$$

Where v_{doi}, r_{ci} and $\boldsymbol{\phi}_i$ are expressed as the open circuit DC voltage value, the commutating resistance and the phase angle between the AC voltage and the current at the inverter side, respectively. Figure 6 shows an equivalent circuit of a two terminal HVDC link system [21], [32], [37].

The voltage balance equation of the DC link is defined as follows:

$$v_{dr} - v_{di} - r_{dc} i_d = 0 \tag{18}$$

TABLE 4. Composite benchmark test functions.

Function	Dim	Range
f_{24} (CF_1) $f_1, f_2, f_3, f_4, \ldots, f_{10}$=Sphere Function $[\sigma_1,\sigma_2,\sigma_3,\sigma_4,\ldots,\sigma_{10}]=[1,1,1,1,\ldots,1]$ $[\lambda_1,\lambda_2,\lambda_3,\lambda_4,\ldots,\lambda_{10}]=[5/100,5/100,5/100,5/100,\ldots,5/100]$	10	[-5,5]
f_{25} (CF_2) $f_1, f_2, f_3, f_4, \ldots, f_{10}$=Griewank's Function $[\sigma_1,\sigma_2,\sigma_3,\sigma_4,\ldots,\sigma_{10}]=[1,1,1,1,\ldots,1]$ $[\lambda_1,\lambda_2,\lambda_3,\lambda_4,\ldots,\lambda_{10}]=[5/100,5/100,5/100,5/100,\ldots,5/100]$	10	[-5,5]
f_{26} (CF_3) $f_1, f_2, f_3, f_4, \ldots, f_{10}$=Griewank's Function $[\sigma_1,\sigma_2,\sigma_3,\sigma_4,\ldots,\sigma_{10}]=[1,1,1,1,\ldots,1]$ $[\lambda_1,\lambda_2,\lambda_3,\lambda_4,\ldots,\lambda_{10}]=[1,1,1,1,\ldots,1]$	10	[-5,5]
f_{27} (CF_4) f_1, f_2= Ackley's Function f_3, f_4= Rastrigin's Function f_5, f_6= Weierstrass Function f_7, f_8= Griewank's Function f_9, f_{10}= Sphere Function $[\sigma_1,\sigma_2,\sigma_3,\sigma_4,\ldots,\sigma_{10}]=[1,1,1,1,\ldots,1]$ $[\lambda_1,\lambda_2,\lambda_3,\lambda_4,\ldots,\lambda_{10}]=[5/32,5/32,1,1,5/0.5,5/0.5,5/100,5/100,5/100,5/100]$	10	[-5,5]
f_{28} (CF_5) f_1, f_2= Rastrigin's Function f_3, f_4= Weierstrass Function f_5, f_6= Griewank's Function f_7, f_8= Ackley's Function f_9, f_{10}= Sphere Function $[\sigma_1,\sigma_2,\sigma_3,\sigma_4,\ldots,\sigma_{10}]=[1,1,1,1,\ldots,1]$ $[\lambda_1,\lambda_2,\lambda_3,\lambda_4,\ldots,\lambda_{10}]=[1/5,1/5,5/0.5,5/0.5,5/100,5/100,5/32,5/32,5/100,5/100]$	10	[-5,5]
f_{29} (CF_6) f_1, f_2= Rastrigin's Function f_3, f_4= Weierstrass Function f_5, f_6= Griewank's Function f_7, f_8= Ackley's Function f_9, f_{10}= Sphere Function $[\sigma_1,\sigma_2,\sigma_3,\sigma_4,\ldots,\sigma_{10}]=[0.1,0.2,0.3,0.4,0.5,0.6,0.7,0.8,0.9,1]$ $[\lambda_1,\lambda_2,\lambda_3,\lambda_4,\ldots,\lambda_{10}]=[0.1\times1/5, 0.2\times1/5, 0.3\times5/0.5, 0.4\times5/0.5, 0.5\times5/100,$ $0.6\times5/100, 0.7\times5/32, 0.8\times5/32, 0.9\times5/100, 1\times5/100]$	10	[-5,5]

TABLE 5. Comparison of the obtained optimization results for the unimodal test functions.

Test Functions		MSA	MSA-AC	TLBO	FA	SSA	DA	MVO
f_1	Best	0.0000	**0.0000**	9.1174×10^{-180}	1.0553×10^{-16}	5.0355×10^{-9}	1231.9927	0.11302
	Mean	2.4871×10^{-313}	$\mathbf{1.2747\times10^{-321}}$	1.1688×10^{-177}	1.4857×10^{-16}	9.0177×10^{-9}	4370.3952	0.17576
	Max.	7.4613×10^{-312}	$\mathbf{2.7678\times10^{-320}}$	9.1934×10^{-177}	1.7745×10^{-16}	1.2569×10^{-8}	9484.9196	0.36614
	Std.	0.0000	**0.0000**	0.0000	1.17481×10^{-17}	1.8408×10^{-9}	2006.9072	0.051051
f_2	Best	1.3288×10^{-178}	$\mathbf{2.1375\times10^{-181}}$	2.141×10^{-89}	4.198×10^{-9}	0.013287	19.62398	0.15925
	Mean	1.0921×10^{-162}	$\mathbf{3.6662\times10^{-163}}$	1.4114×10^{-88}	5.1763×10^{-9}	0.68743	53.96757	0.28009
	Max.	1.6966×10^{-161}	$\mathbf{1.0946\times10^{-161}}$	5.2656×10^{-88}	5.7205×10^{-9}	3.9352	152.1796	0.5821
	Std.	3.8499×10^{-162}	$\mathbf{2.2228\times10^{-162}}$	1.2876×10^{-88}	3.609×10^{-10}	0.93587	32.32264	0.080808
f_3	Best	8.1964×10^{-287}	$\mathbf{4.7108\times10^{-294}}$	3.1211×10^{-40}	8.3206×10^{-16}	5.039997	10687.5235	8.17298
	Mean	1.6310×10^{-253}	$\mathbf{1.1288\times10^{-263}}$	7.1968×10^{-36}	1.557×10^{-15}	53.59656	28105.2916	15.9378
	Max.	2.8980×10^{-252}	$\mathbf{3.3762\times10^{-262}}$	2.0231×10^{-34}	2.608×10^{-15}	382.5653	56833.7564	28.3545
	Std.	0.0000	**0.0000**	3.6871×10^{-35}	4.3062×10^{-16}	70.79741	11457.4296	5.29582
f_4	Best	1.6925×10^{-163}	$\mathbf{8.3920\times10^{-165}}$	1.3249×10^{-72}	4.2747×10^{-9}	0.254226	19.1489	0.28031
	Mean	4.4364×10^{-149}	$\mathbf{9.6103\times10^{-154}}$	2.2326×10^{-71}	5.5894×10^{-9}	4.49811	34.1908	0.64786
	Max.	1.3049×10^{-147}	$\mathbf{2.3668\times10^{-152}}$	1.5478×10^{-70}	6.6634×10^{-9}	10.9091	53.8963	1.6255
	Std.	2.3813×10^{-148}	$\mathbf{4.3351\times10^{-153}}$	3.2432×10^{-71}	5.2751×10^{-10}	2.91214	7.97702	0.31237
f_5	Best	25.9945	**25.8823**	26.4649	34.10554	30.8394399	1339.471555	26.778073
	Mean	27.3103	**27.1001**	27.2333	57.25647	792.944204	31225.15233	360.72766
	Max.	28.7298	28.1159	**27.9772**	188.354	15193.2096	200095.3543	2025.0989
	Std.	0.831988	0.550005	**0.399805**	41.34033	2735.10896	47680.83751	554.51034
f_6	Best	2.1120×10^{-4}	$\mathbf{1.3181\times10^{-4}}$	0.017723	0.7059	7.9171×10^{-4}	1194.76103	0.11228
	Mean	7.5016×10^{-4}	$\mathbf{6.1906\times10^{-5}}$	0.070395	0.91439	0.169	4504.58756	0.18331
	Max.	$\mathbf{2.4295\times10^{-3}}$	2.5672×10^{-3}	0.21617	1.1415	1.8597	12749.9735	0.25448
	Std.	6.3684×10^{-4}	$\mathbf{4.6526\times10^{-4}}$	0.043119	0.11806	0.35765	2213.91666	0.040745
f_7	Best	2.4313×10^{-5}	$\mathbf{2.8178\times10^{-6}}$	1.364×10^{-4}	3.4327×10^{-4}	2.8877×10^{-2}	7.7823×10^{-2}	6.0525×10^{-3}
	Mean	1.9818×10^{-4}	$\mathbf{1.8093\times10^{-4}}$	4.6051×10^{-4}	7.1481×10^{-4}	4.9677×10^{-2}	1.6997	1.3665×10^{-2}
	Max.	5.8547×10^{-4}	$\mathbf{5.5394\times10^{-4}}$	9.9052×10^{-4}	1.0727×10^{-3}	1.1829×10^{-1}	5.6903	2.9432×10^{-2}
	Std.	1.3809×10^{-4}	$\mathbf{1.2224\times10^{-4}}$	2.157×10^{-4}	2.2027×10^{-4}	2.0144×10^{-2}	1.4101	5.4618×10^{-3}

1) OBJECTIVE FUNCTIONS

The objective function of the OPF problem of two-terminal HVDC systems can be expressed as the minimization of the fuel cost of the generating units.

- *First objective function*

The first objective function is mathematically described as follows:

$$f(x,u)=\sum_{i=1}^{NG}\left(a_iP_{Gi}^2+b_iP_{Gi}+c_i\right) \tag{19}$$

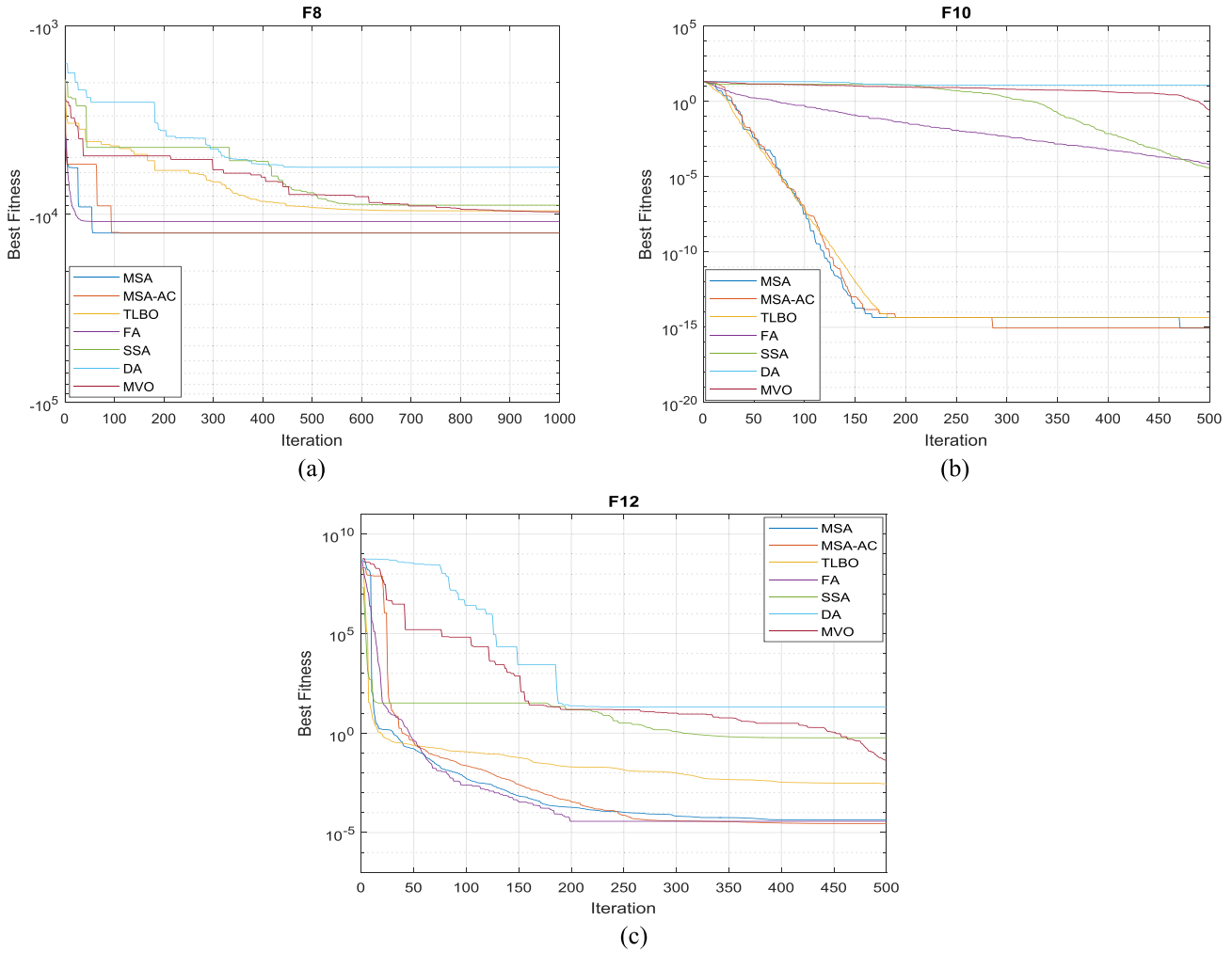

FIGURE 3. Convergence curves of the proposed MSA-AC and the other optimization algorithms for the multimodal test functions.

Where P_{Gi}, a_i, b_i and c_i are specified as the active power output and the cost coefficients of the ith generating unit.

- *Second objective function*

Voltage deviation is depicted as the voltage quality in the power system. The voltage deviation index is one of the most significant safety and qualification indices. In this study, the voltage deviation is defined as single objective function. It is mathematically explained as follow:

$$f(x,u) = VD = \left(\sum_{j=1}^{NPQ} \left| V_{L_j} - 1 \right| \right) \tag{20}$$

- *Third objective function:*

Modern power systems are comprised of long transmission lines and heavy loading. This situation reveals the voltage stability problem. The voltage stability is defined as keeping within the specified bus voltage limit values at each bus in the power system under nominal operating conditions. Improvement of voltage stability of a power system is one of the most important parameter of the modern power system operation and planning. L-index values of each bus in the modern power systems are a good indicator for the definition of power system voltage stability [29].

L-index value gets the changing values from 0 to 1. 0 and 1 values are defined as no load case and the voltage collapse, respectively [29].

$$L_j = \left| 1 - \sum_{i=1}^{NG} F_{ji} \frac{V_i}{V_j} \right|, \quad where \quad j = 1, 2, \ldots, NPQ$$

$$F_{ji} = -\left[Y_1 \right]^{-1} \left[Y_2 \right] \tag{21}$$

Y_1 and Y_2 are the sub-matrices of the system YBUS matrix obtained after separating the PQ and PV buses parameters as depicted in the following equation:

$$\begin{bmatrix} I_L \\ I_G \end{bmatrix} = \begin{bmatrix} Y_1 & Y_2 \\ Y_3 & Y_4 \end{bmatrix} \begin{bmatrix} V_L \\ V_G \end{bmatrix} \tag{22}$$

L-index is computed for all the load buses. The maximum value of L-index is calculated as global system indicator for

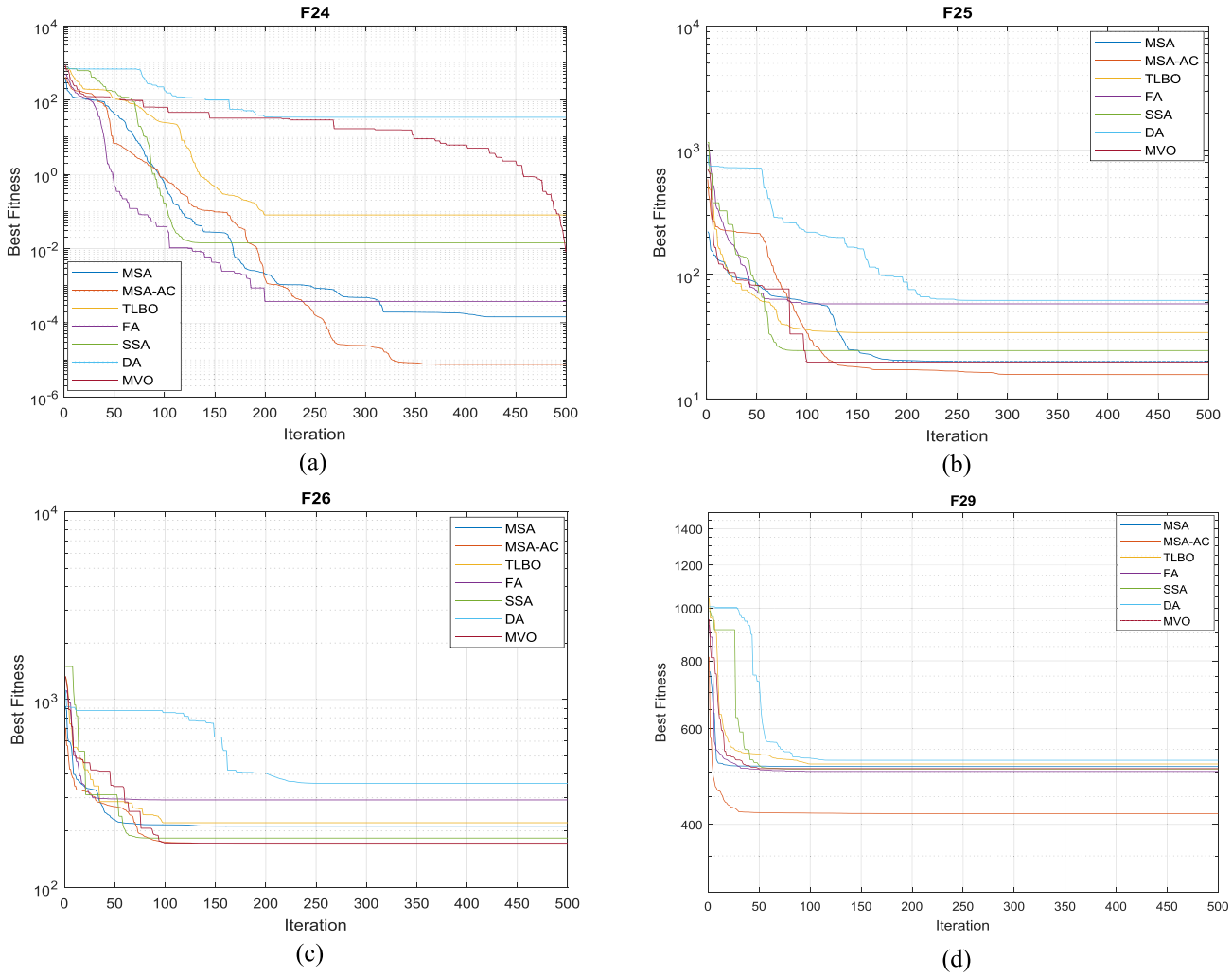

FIGURE 4. Convergence curves of the proposed MSA-AC and the other optimization algorithms for the composite test functions.

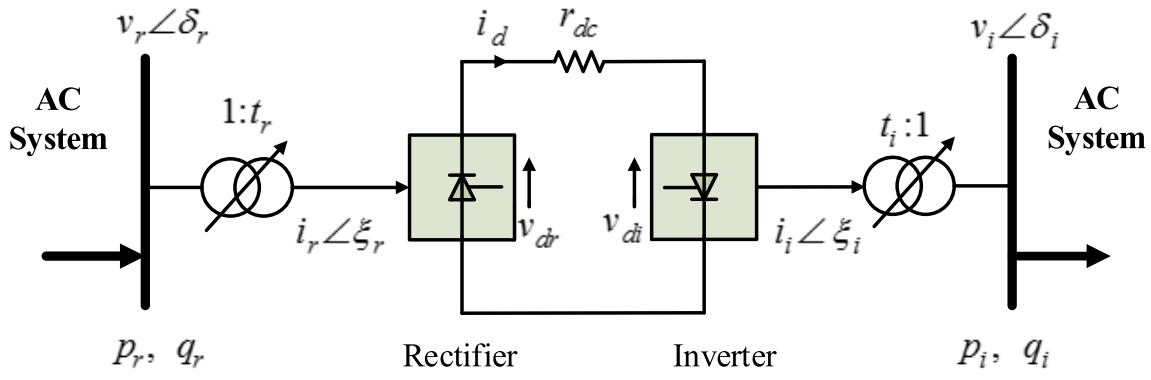

FIGURE 5. A two terminal AC-DC transmission system.

the power system stability. It is expressed as follows:

$$f(x,u) = L_{\max} = \max\left(L_j\right), \quad where\ j = 1, 2, \ldots, NPQ \tag{23}$$

2) EQUALITY CONSTRAINTS

Figure 7 shows the AC bus connected with the DC transmission link [21], [32], [37]. The mathematical equations belonging to this system are expressed as the

TABLE 6. Comparison of the obtained optimization results for the multimodal test functions.

Test Functions		MSA	MSA-AC	TLBO	FA	SSA	DA	MVO
f_8	Best	-12569.4866	**-12569.4866**	-9584.3921	-10928.0528	-8941.4885	-5624.7711	-9704.5769
	Mean	-12514.7968	**-12564.17**	-8418.6042	-9422.97521	-7536.9625	-4618.0356	-7740.5742
	Max.	-11066.8977	**-12550.088**	-6730.4765	-8297.87767	-6147.0732	-3412.0029	-6345.1337
	Std.	274.310045	**4.27348687**	722.95117	595.382506	753.30254	577.75484	759.93189
f_9	Best	0.0000	**0.0000**	0.0000	27.8588	15.9193	93.55987	48.81803
	Mean	0.0000	**0.0000**	9.52998	49.9137	47.1941	236.3819	114.147
	Max.	0.0000	**0.0000**	31.8394	94.5208	77.6067	312.6994	195.0768
	Std.	0.0000	**0.0000**	6.75413	17.8348	16.1528	56.12311	33.82126
f_{10}	Best	8.8818×10^{-16}	$\mathbf{8.8818\times10^{-16}}$	4.4409×10^{-15}	6.5797×10^{-5}	3.6406×10^{-5}	11.9404	0.2629
	Mean	1.125×10^{-15}	$\mathbf{1.125\times10^{-15}}$	6.6909×10^{-15}	7.7932×10^{-5}	2.0061	14.8391	1.6005
	Max.	4.4409×10^{-15}	$\mathbf{4.4409\times10^{-15}}$	7.9936×10^{-15}	8.8655×10^{-5}	4.6238	16.8529	3.0772
	Std.	9.0135×10^{-16}	$\mathbf{9.0135\times10^{-16}}$	1.7413×10^{-16}	5.8925×10^{-6}	1.0103	1.35399	0.7715
f_{11}	Best	0.0000	**0.0000**	0.0000	1.4643×10^{-7}	9.1718×10^{-6}	34.74325	0.55419
	Mean	0.0000	**0.0000**	0.0000	2.3821×10^{-3}	1.0635×10^{-2}	70.50943	0.72321
	Max.	0.0000	**0.0000**	0.0000	1.7227×10^{-2}	6.4091×10^{-2}	116.7616	0.92688
	Std.	0.0000	**0.0000**	0.0000	4.6865×10^{-3}	1.4935×10^{-2}	24.3862	0.10021
f_{12}	Best	4.4392×10^{-5}	$\mathbf{2.8257\times10^{-5}}$	2.7614×10^{-3}	3.6801×10^{-5}	0.58186	20.33271	4.2877×10^{-2}
	Mean	3.5366×10^{-3}	$\mathbf{8.0606\times10^{-5}}$	1.8659×10^{-2}	0.14207	4.531	1086348.4744	1.87
	Max.	0.10385	$\mathbf{1.2709\times10^{-4}}$	6.6679×10^{-2}	1.4557	9.2009	7698367.9643	4.933
	Std.	0.018947	$\mathbf{2.4679\times10^{-5}}$	1.5824×10^{-2}	0.32137	2.3966	1840823.7576	1.2236
f_{13}	Best	5.9429×10^{-4}	$\mathbf{3.3766\times10^{-4}}$	5.9831×10^{-4}	6.2993×10^{-4}	8.39183×10^{-3}	412036.285485	0.037522
	Mean	4.6954×10^{-2}	2.4585×10^{-2}	0.25351	$\mathbf{9.0887\times10^{-4}}$	13.8521	7680914.19762	0.12329
	Max.	0.25185	0.14450	0.8571	$\mathbf{1.28\times10^{-3}}$	37.6828	34128568.3116	0.47652
	Std.	0.062036	0.036214	0.19116	$\mathbf{1.4599\times10^{-4}}$	11.3744	8648398.23377	0.10345

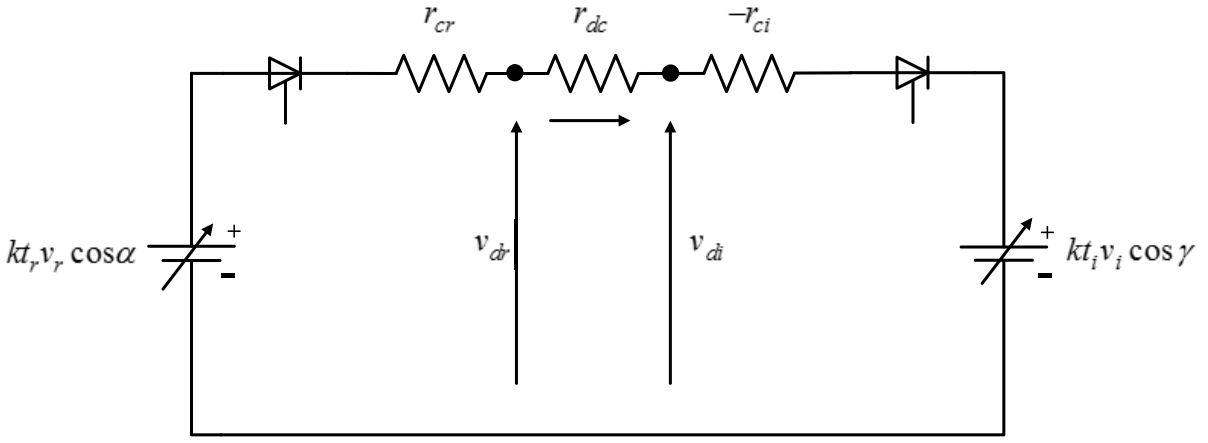

FIGURE 6. The equivalent circuit of a two terminal HVDC link system.

kth bus.

$$p_{gk} - p_{lk} - p_{dk} - p_k = 0 \tag{24}$$

$$q_{gk} + q_{sk} - q_{lk} - q_{dk} - q_k = 0 \tag{25}$$

Where p_{gk}, p_{lk}, p_{dk} and p_k are depicted as active powers of the generating unit, load bus, DC link and kth bus, respectively. q_{gk}, q_{sk}, q_{lk}, q_{dk} and q_k are defined as reactive powers of the generating unit, shunt compensator, load bus, DC link and kth bus, respectively.

The active and reactive equations of the kth bus are expressed as follows:

$$p_k = v_k \sum_{j=1}^{N} v_j \left(G_{kj} \cos\delta_{kj} + B_{kj} \sin\delta_{kj}\right) \tag{26}$$

$$q_k = v_k \sum_{j=1}^{N} v_j \left(G_{kj} \sin\delta_{kj} - B_{kj} \cos\delta_{kj}\right) \tag{27}$$

Where v_k and v_j are the voltage magnitude of kth and jth bus, respectively. G_{kj}, B_{kj} and δ_{kj} are defined as the conductance, susceptance, voltage angle difference between kth and jth bus, respectively. The power equations of the rectifier and inverter connected with busses are depicted as follows [21]:

$$\begin{aligned} p_{dk} &= p_r \\ q_{dk} &= q_r \\ p_{dk} &= -p_i \\ q_{dk} &= q_i \end{aligned} \tag{28}$$

3) INEQUALITY CONSTRAINTS

The terminal voltage magnitude, the active and reactive power output of the generating units, the voltage value of all the load busses, the transformer tap settings and DC transmission link limitations are expressed by the minimum and

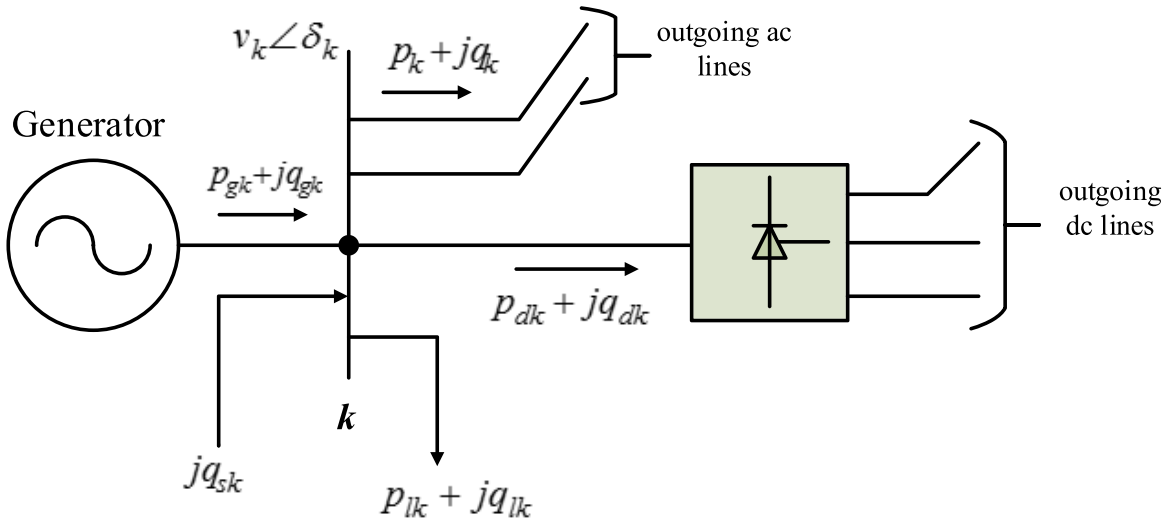

FIGURE 7. The AC bus connected with the DC transmission link.

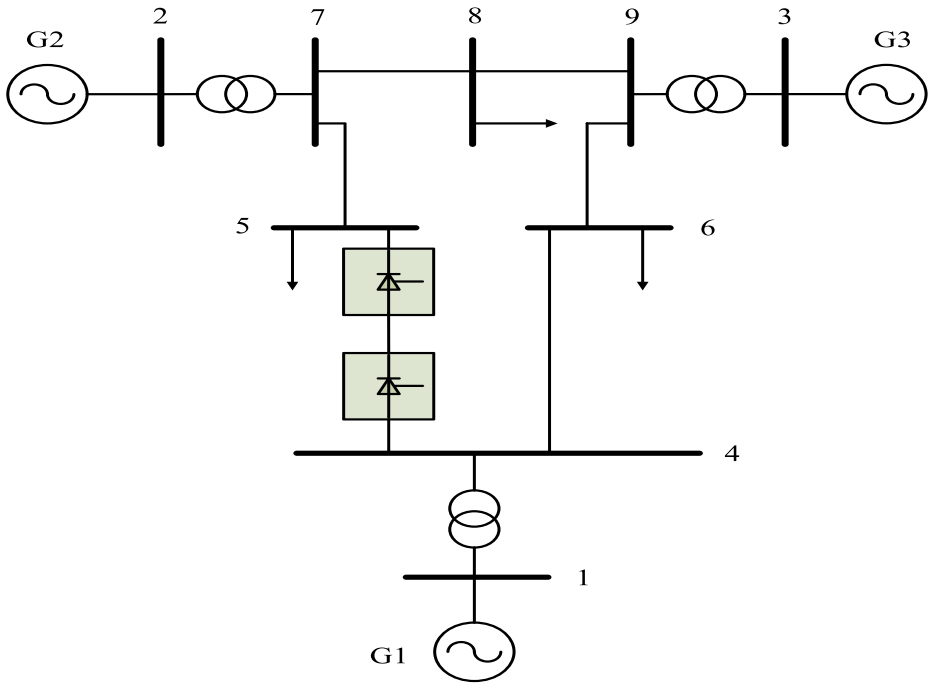

FIGURE 8. The test system 1.

maximum limit values, respectively [21].

$$\begin{aligned}
P_{Gi}^{\min} &\le P_{Gi} \le P_{Gi}^{\max} \quad i = 1, \ldots, NG \\
Q_{Gi}^{\min} &\le Q_{Gi} \le Q_{Gi}^{\max} \quad i = 1, \ldots, NG \\
V_{Gi}^{\min} &\le V_{Gi} \le V_{Gi}^{\max} \quad i = 1, \ldots, NG \\
V_{Li}^{\min} &\le V_{Li} \le V_{Li}^{\max} \quad i = 1, \ldots, NPQ \\
T_i^{\min} &\le T_i \le T_i^{\max} \quad i = 1, \ldots, NT \\
i_d^{\min} &\le i_d \le i_d^{\max} \\
p_{dk}^{\min} &\le p_{dk} \le p_{dk}^{\max} \quad k = 1, 2
\end{aligned} \tag{29}$$

$$\begin{aligned}
q_{dk}^{\min} &\le q_{dk} \le q_{dk}^{\max} \quad k = 1, 2 \\
t_{dk}^{\min} &\le t_{dk} \le t_{dk}^{\max} \quad k = 1, 2 \\
v_{dk}^{\min} &\le v_{dk} \le v_{dk}^{\max} \quad k = 1, 2 \\
\alpha^{\min} &\le \alpha \le \alpha^{\max} \\
\gamma^{\min} &\le \gamma \le \gamma^{\max}
\end{aligned} \tag{30}$$

The objective function including penalty factors can be expressed as follows. λ_1, λ_2, λ_3, λ_4, λ_5, λ_6, λ_7, λ_8 and

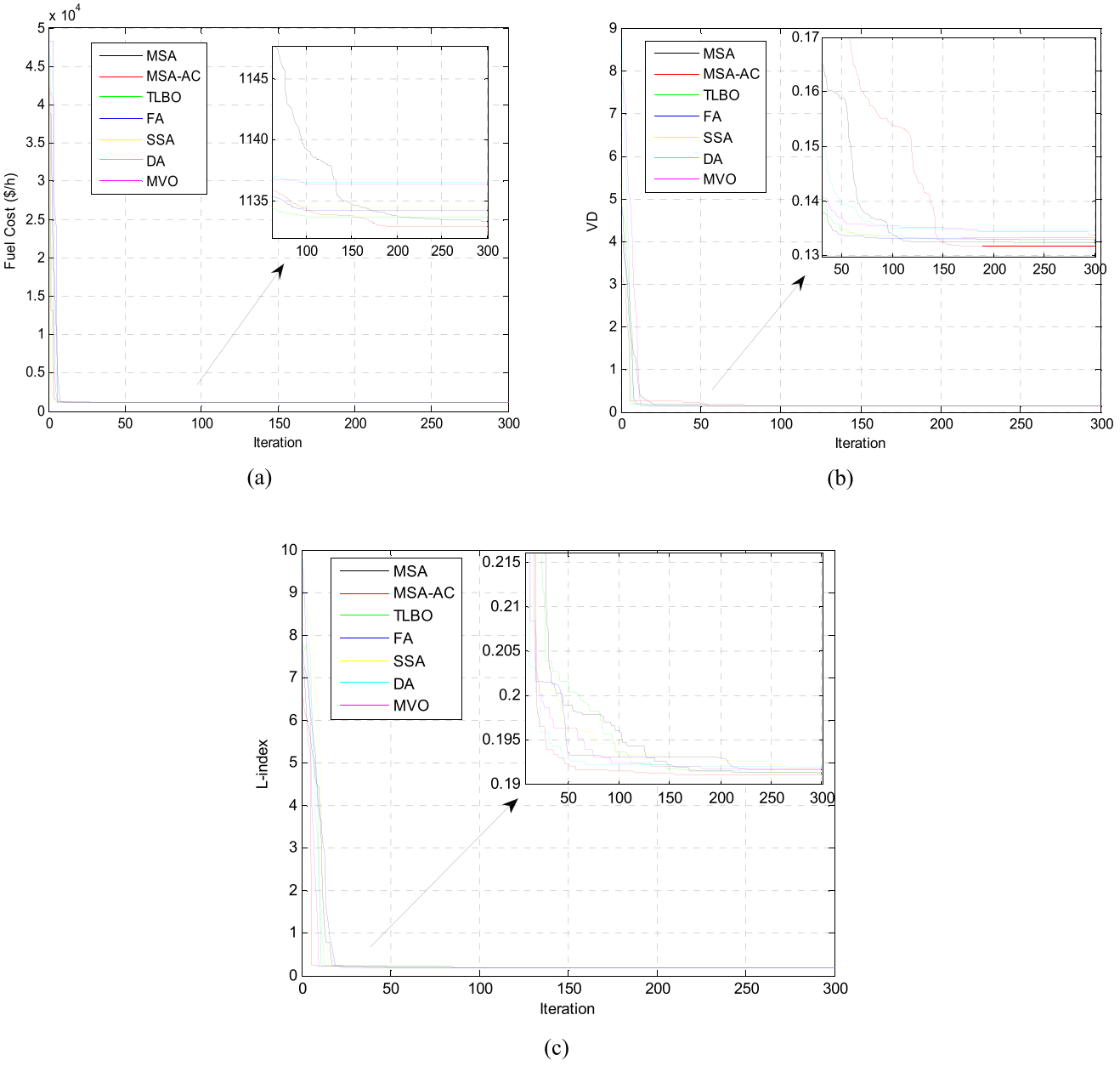

FIGURE 9. Comparative convergence curves of the MSA-AC and the other methods for test system 1.

λ_9 are defined as penalty coefficients [21], [32], [37].

$$J = f(x,u) + \lambda_1 \left| P_{G_{slack}} - P^{\lim}_{G_{slack}} \right| + \lambda_2 \sum_{i=1}^{NPQ} \left| V_{Li} - V^{\lim}_{Li} \right| + \lambda_3 \sum_{i=1}^{NG} \left| Q_{Gi} - Q^{\lim}_{Gi} \right| + \lambda_4 \left| t_r - t^{\lim}_r \right| + \lambda_5 \left| t_i - t^{\lim}_i \right| + \lambda_6 \left| \alpha - \alpha^{\lim} \right| + \lambda_7 \left| \gamma - \gamma^{\lim} \right| + \lambda_8 \left| v_{dr} - v^{\lim}_{dr} \right| + \lambda_9 \left| v_{di} - v^{\lim}_{di} \right| \quad (31)$$

Both the MSA and the proposed MSA-AC algorithms were investigated for solving the OPF problem with two-terminal HVDC systems. These methods were applied on two different systems: the modified New England 39-bus and the modified WSCC 9-bus test systems. All data of these test systems were obtained from references [21], [32], [37]. The power flow calculations were carried out via the 6.0b2 MATPOWER package [42], [43].

4) APPLICATION OF MSA-AC METHOD TO SOLVE OPF PROBLEM WITH TWO-TERMINAL HVDC SYSTEM

In this section, application of the proposed MSA-AC method for solving the OPF problem with two-terminal HVDC systems is presented. According to the number of the initial population (N) of the algorithm, the independent or control variables of this problem were generated as candidate solutions within the specified minimum and maximum values.

TABLE 7. Comparison of the obtained optimization results for the multimodal low-dimensional test functions.

Test Functions		MSA	MSA-AC	TLBO	FA	SSA	DA	MVO
f_{14}	Best	0.998004	0.998004	**0.998**	0.998	0.998	0.998004	0.998
	Mean	2.72716	2.17293	**1.1633**	1.0311	1.1631	4.98221	1.1965
	Max.	12.6705	10.7632	**3.9683**	1.992	3.9683	19.2307	2.9821
	Std.	3.50956	2.97387	**0.64164**	0.18148	0.64168	5.78192	0.54668
f_{15}	Best	3.0759×10^{-4}	$\mathbf{3.0749\times10^{-4}}$	3.4098×10^{-4}	3.1095×10^{-4}	4.1216×10^{-4}	7.0306×10^{-4}	3.1984×10^{-4}
	Mean	1.9259×10^{-3}	$\mathbf{1.2145\times10^{-3}}$	3.0185×10^{-3}	2.2378×10^{-3}	1.4765×10^{-3}	1.436×10^{-2}	3.4095×10^{-3}
	Max.	2.0416×10^{-2}	2.0717×10^{-2}	$\mathbf{2.0363\times10^{-2}}$	2.0363×10^{-2}	2.0363×10^{-2}	9.8968×10^{-2}	2.0363×10^{-2}
	Std.	5.0316×10^{-3}	3.6982×10^{-3}	5.978×10^{-3}	5.002×10^{-3}	$\mathbf{3.5763\times10^{-3}}$	2.3572×10^{-2}	6.7709×10^{-3}
f_{16}	Best	-1.0316	**-1.0316**	-1.0316	-1.0316	-1.0316	-1.0316	-1.0316
	Mean	-0.92281	**-1.0316**	-1.0316	-1.0316	-1.0316	-1.0316	-1.0316
	Max.	-0.21546	**-1.0316**	-1.0316	-1.0316	-1.0316	-1.0316	-1.0316
	Std.	0.28219	$\mathbf{6.2532\times10^{-16}}$	6.7752×10^{-16}	1.3034×10^{-9}	1.543×10^{-14}	5.2174×10^{-5}	2.035×10^{-7}
f_{17}	Best	0.39789	**0.39789**	0.39789	0.39789	0.39789	0.39789	0.39789
	Mean	0.39789	**0.39789**	0.39789	0.39789	0.39789	0.398	0.39789
	Max.	0.39789	**0.39789**	0.39789	0.39789	0.39789	0.40026	0.39789
	Std.	4.5074×10^{-16}	$\mathbf{3.2434\times10^{-16}}$	2.2704×10^{-15}	1.6198×10^{-9}	1.6596×10^{-14}	4.3247×10^{-4}	5.1811×10^{-7}
f_{18}	Best	3.0	**3.0**	3.0	3.0	3.0	3.0	3.0
	Mean	4.8	**4.8**	9.3	6.6	5.70102	5.70006	5.70144
	Max.	30	**30**	84	84	84.0305	84	84.0004
	Std.	6.85012	**6.85012**	16.9037	15.4264	14.7941	14.7885	14.7883
f_{19}	Best	-3.8628	**-3.8628**	-3.8628	-3.8628	-3.8628	-3.8628	-3.8628
	Mean	-3.8628	**-3.8628**	-3.8628	-3.8628	-3.8628	-3.8229	-3.8628
	Max.	-3.8628	**-3.8628**	-3.8627	-3.8628	-3.8626	-3.0891	-3.8628
	Std.	2.4397×10^{-9}	$\mathbf{1.3713\times10^{-9}}$	1.9791×10^{-5}	7.8352×10^{-9}	3.9915×10^{-5}	0.14424	1.7126×10^{-6}
f_{20}	Best	-3.322	**-3.322**	-3.322	-3.322	-3.322	-3.3213	-3.322
	Mean	-3.2546	**-3.2863**	-3.2836	-3.2665	-3.2124	-3.2461	-3.2463
	Max.	-3.2028	-3.2029	-3.2023	**-3.2031**	-3.0406	-2.9364	-3.2004
	Std.	0.059944	**0.055442**	0.055627	0.060328	0.082299	0.10106	0.058618
f_{21}	Best	-10.1532	**-10.1532**	-10.1532	-10.1532	-10.1532	-10.0699	-10.1531
	Mean	-9.90243	**-10.1532**	-7.38582	-8.7325	-6.63232	-5.30575	-6.69927
	Max.	-2.63047	**-10.1532**	-2.63046	-2.68286	-2.63047	-2.52275	-2.63045
	Std.	1.37346	$\mathbf{2.72185\times10^{-7}}$	2.97306	2.6844	3.26573	2.77477	2.99522
f_{22}	Best	-10.4029	**-10.4029**	-10.4029	-10.4029	-10.4029	-10.3736	-10.4029
	Mean	-8.5254	**-9.10961**	-8.80631	-6.50222	-8.98531	-5.46357	-8.42527
	Max.	-1.83759	**-2.7659**	-2.7659	-1.83759	-2.75193	-2.72262	-2.76588
	Std.	3.18164	**2.70668**	2.79876	3.74931	2.91166	2.92672	3.14035
f_{23}	Best	-10.5364	**-10.5364**	-10.5364	-10.5364	-10.5364	-10.5358	-10.5363
	Mean	-9.58746	**-10.0897**	-7.9080	-6.30535	-7.5219	-5.73117	-9.18742
	Max.	-2.80663	**-3.83543**	-2.42734	-1.85948	-2.42173	-1.66084	-2.42733
	Std.	2.31463	**1.70009**	3.2981	3.79297	3.79246	3.76442	2.52999

TABLE 8. Comparison of the obtained optimization results for the composite test functions.

Test Functions		MSA	MSA-AC	TLBO	FA	SSA	DA	MVO
f_{24}	Best	1.43976×10^{-4}	$\mathbf{7.547287\times10^{-6}}$	8.008909×10^{-2}	3.709864×10^{-4}	1.418499×10^{-2}	34.34194	8.189192×10^{-3}
	Mean	86.667	90.00037	100.6449	**76.66709**	103.5806	190.3243	140.0148
	Max.	300	300	401.0038	**200.0005**	403.3172	394.4253	600.0042
	Std.	81.93053	80.30104	105.5043	**77.38533**	115.3973	87.74848	145.2671
f_{25}	Best	19.93787	**15.62415**	34.0597	57.95274	24.39715	61.82261	19.67429
	Mean	157.4898	**130.3947**	218.7591	276.3771	253.3667	235.1397	249.6802
	Max.	499.1522	**331.1712**	498.9442	510.5832	534.2996	715.0616	444.8332
	Std.	110.3563	**80.75312**	145.4877	123.2829	157.631	141.6822	115.962
f_{26}	Best	211.6915	**169.9463**	221.0781	292.2129	183.18919	358.03305	172.5651
	Mean	361.9499	**356.8006**	427.1891	531.1223	486.45314	716.71429	370.2963
	Max.	627.7023	**594.7050**	701.2673	876.1064	1208.8755	1044.2146	701.9902
	Std.	115.4485	**104.6696**	151.7667	168.3029	223.31228	207.53928	126.4839
f_{27}	Best	360.1739	**316.9145**	346.5947	386.3835	317.9786	412.31521	327.6261
	Mean	566.2432	516.2881	663.525	590.0504	524.3917	666.45958	**510.7322**
	Max.	767.5403	**754.0959**	918.0768	800.0114	821.8632	1053.0569	800.0462
	Std.	140.2033	**123.5580**	177.684	122.7633	153.9201	130.5144	151.4973
f_{28}	Best	27.4978	**27.49425**	67.82356	61.711631	34.90506	315.14833	28.181563
	Mean	162.4861	**132.4923**	229.5381	316.32145	273.0737	672.43451	290.71178
	Max.	545.8664	**253.2745**	554.1031	1006.2691	558.7867	1024.1486	1024.9002
	Std.	157.1349	**69.2079**	121.3344	194.75978	183.7285	212.98624	231.91152
f_{29}	Best	511.0277	**418.469**	516.6406	500.6354	505.9504	524.8948	506.5764
	Mean	785.1252	**756.5143**	825.9153	765.8238	776.4312	874.92	830.0309
	Max.	900	**900**	908.7093	906.3592	917.2101	927.6317	918.2195
	Std.	179.8482	168.3135	154.3778	191.1864	180.392	**110.8775**	161.3804

The mathematical equation applied is shown as follows:

$$init_p op_i = rand_i[0,1] \times (UB_{1\times d} - LB_{1\times d}) + LB_{1\times d} \quad i = 1, 2, 3, \ldots, N \qquad (32)$$

Where UB, LB and d are defined as the upper limit values of the control variables, the lower limit values of the control variables and the number of the of the control variables, respectively. The initial population within the specified limit

TABLE 9. Comparative results by the proposed MSA-AC and the other methods (for the fuel cost of the test system I).

Variable	MSA-AC	MSA	TLBO	FA	SSA	DA	MVO	BSA[21]	GA[37]
P_{G1}	1.067552	1.072710	1.081022	1.081902	1.099721	1.115515	1.114308	1.07118	0.96905
P_{G2}	1.125302	1.124660	1.104517	1.089576	1.097257	1.087407	1.091687	1.13236	1.22509
P_{G3}	0.991339	0.988244	1.000698	1.016145	0.990904	0.990471	0.987053	0.98724	1.02942
Q_{G1}	0.141405	0.145475	0.232104	0.224324	0.251640	0.297792	0.264119	0.20760	0.01092
Q_{G2}	0.539248	0.553110	0.539229	0.532912	0.554534	0.582504	0.602579	0.58083	0.70183
Q_{G3}	-0.204530	-0.152152	-0.223459	-0.151763	-0.185298	-0.150952	-0.128614	-0.10439	-0.13526
V_1	0.9271	1.0798	1.0484	0.9662	1.0417	0.9723	1.0611	0.941	1.063640
V_2	0.9708	1.0406	0.9596	0.9579	0.9603	0.9643	0.9941	1.010	1.083900
V_3	0.9537	1.0829	1.0696	0.9481	0.9643	0.9325	1.1000	1.012	1.061280
V_4	1.0758	1.0681	1.0867	1.0787	1.0831	1.0781	1.0701	1.036	1.047477
V_5	0.9987	0.9949	0.9960	0.9902	0.9934	0.9907	0.9886	0.919	0.924871
V_6	1.0697	1.0651	1.0771	1.0724	1.0755	1.0715	1.0660	1.025	1.034400
V_7	1.1000	1.0999	1.0990	1.0967	1.0999	1.0998	1.1000	1.037	1.047932
V_8	1.0870	1.0878	1.0873	1.0869	1.0891	1.0892	1.0889	1.028	1.034598
V_9	1.0941	1.0963	1.0963	1.0987	1.0993	1.1000	1.0991	1.045	1.046922
T_{1-4}	0.8569	1.0051	0.9554	0.8873	0.9515	0.8903	0.9802	0.9000	1.016165
T_{2-7}	0.8606	0.9216	0.8513	0.8517	0.8506	0.8531	0.8785	0.9451	0.998110
T_{3-9}	0.8817	0.9964	0.9877	0.8705	0.8863	0.8550	1.0083	0.9757	1.022753
p_{dr}	0.7338	0.7826	0.8641	0.8817	0.9119	1.0296	1.0102	0.7107	0.136029
p_{di}	0.7335	0.7822	0.8637	0.8812	0.9114	1.0289	1.0095	0.7103	0.136019
q_{dr}	0.1619	0.1917	0.1916	0.2193	0.2275	0.2639	0.26606	0.1635	0.024080
q_{di}	0.1660	0.1979	0.2067	0.2267	0.2375	0.2774	0.2845	0.1804	0.026697
i_d	0.4990	0.6571	0.5817	0.7207	0.7409	0.8334	0.8260	1.2298	0.100000
t_r	1.0364	0.8501	1.0368	0.8654	0.8673	0.8760	0.8739	0.9025	0.976568
t_i	1.1174	0.9139	1.1350	0.9441	0.9476	0.9558	0.9510	1.0222	1.109794
α (^{o})	9.9705	9.9858	9.6155	9.9685	9.9187	9.8622	9.9907	9.5529	9.417373
γ (^{o})	10.0003	10.0261	10.4461	10.0129	10.1575	10.2188	11.1609	10.8126	10.474138
v_{dr}	1.4704	1.1911	1.4854	1.2234	1.2309	1.2354	1.2229	1.2304	-
v_{di}	1.4699	1.1904	1.4848	1.2227	1.2301	1.2346	1.2221	1.2298	-
VD	0.4280	0.4223	0.4504	0.4431	0.4535	0.4479	0.4354	-	-
L_index	0.2172	0.2169	0.2069	0.2106	0.2077	0.2044	0.2084	-	-
Ploss (MW)	3.3944	3.5181	3.5900	3.7104	3.7332	4.2699	4.2366	-	-
Fuel Cost ($/h)	**1132.8925**	1133.3953	1133.719	1134.2706	1134.4888	1136.5176	1136.3679	1135.032	1145.9525

TABLE 10. Comparative results by the proposed MSA-AC and the other methods (for the VD of the test system I).

Variable	MSA-AC	MSA	TLBO	FA	SSA	DA	MVO
P_{G1}	1.478088	1.497139	1.566419	1.535253	1.533051	1.668007	1.357460
P_{G2}	0.117153	0.111832	0.100000	0.613669	0.463577	0.810378	0.100353
P_{G3}	1.620679	1.599484	1.539241	1.046952	1.196159	0.708191	1.786295
Q_{G1}	0.246243	0.285991	0.290270	0.243262	0.304183	0.322433	0.149379
Q_{G2}	0.947478	0.926778	0.923989	80.6992	0.826873	0.792628	1.056595
Q_{G3}	-0.122120	-0.14.8457	-0.153577	-0.213289	-0.215931	-0.239808	-0.051389
V_1	0.9101	0.9011	0.9617	0.9002	0.9002	1.0290	0.9475
V_2	0.9791	0.9965	0.9451	0.9500	0.9186	1.0037	0.9310
V_3	1.0080	0.9058	0.9353	0.9319	0.9216	0.9496	0.9415
V_4	1.0000	1.0015	1.0000	1.0000	1.0000	1.0000	1.0000
V_5	0.9134	0.9122	0.9111	0.9065	0.9063	0.9032	0.9169
V_6	0.9848	0.9858	0.9847	0.9848	0.9848	0.9848	0.9845
V_7	1.0299	1.0288	1.0283	1.0241	1.0244	1.0224	1.0347
V_8	1.0000	1.0000	1.0000	1.0000	1.0000	1.0000	1.0002
V_9	1.0000	1.0000	0.9999	1.0000	1.0000	1.0000	0.9998
T_{1-4}	0.9007	0.8885	0.9497	0.8912	0.8882	1.0150	0.9422
T_{2-7}	0.9028	0.9207	0.8738	0.8874	0.8567	0.9400	0.8502
T_{3-9}	1.0201	0.9181	0.9480	0.9457	0.9360	0.9642	0.9499
p_{dr}	0.6794	0.7670	0.8223	0.7254	0.8325	0.8887	0.4353
p_{di}	0.6791	0.7667	0.8220	0.7251	0.8322	0.8883	0.4352
q_{dr}	0.1515	0.1753	0.1732	0.1399	0.1880	0.1908	0.0844
q_{di}	0.1568	0.1798	0.1965	0.1685	0.1994	0.2166	0.0931
i_d	0.5043	0.5561	0.5974	0.5292	0.6080	0.6519	0.3243
t_r	1.0220	1.0460	1.0417	1.0337	1.0394	1.0325	1.0122
t_i	1.1205	1.1494	1.1499	1.1491	1.1498	1.1499	1.1081
α (^{o})	9.8448	9.9971	8.3956	7.4749	9.4566	8.2890	8.9820
γ (^{o})	10.0101	10.0010	10.0543	10.0086	10.0012	10.0021	10.0630
v_{dr}	1.3471	1.3791	1.3766	1.3707	1.3692	1.3633	1.3421
v_{di}	1.3466	1.3786	1.3760	1.3702	1.3686	1.3627	1.3418
VD	**0.13179**	0.13229	0.13259	0.13287	0.13332	0.13449	0.13367
L_index	0.2645	0.2534	0.2479	0.2630	0.2505	0.2480	0.3024
Ploss (MW)	6.5665	5.8146	5.5303	4.5594	4.2417	3.6151	9.4003
Fuel Cost ($/h)	1260.8888	1258.6178	1259.1657	1173.9441	1188.7436	1173.9281	1282.755

TABLE 11. Comparative results by the proposed MSA-AC and the other methods (for the *L*-Index of the test system I).

Variable	MSA-AC	MSA	TLBO	FA	SSA	DA	MVO
P_{G1}	2.464318	2.470685	2.478342	2.166893	2.370753	2.477780	2.457418
P_{G2}	0.100000	0.105376	0.272120	0.104992	0.100000	0.100000	0.130577
P_{G3}	0.652490	0.655906	0.477022	0.922541	0.739122	0.648173	0.634129
Q_{G1}	0.339536	0.134984	0.150460	0.364977	0.643375	0.226454	0.403735
Q_{G2}	0.875422	0.626866	0.609467	0.935933	1.264297	0.614452	1.101694
Q_{G3}	-0.082434	0.418023	0.394740	-0.322975	-0.677445	0.234734	-0.263663
V_1	0.9004	1.1000	0.9534	0.9001	0.9275	1.0997	0.9616
V_2	0.9755	1.0845	1.0774	0.9783	1.0121	1.0998	1.0161
V_3	0.9000	1.0749	1.0584	0.9780	0.9305	1.0671	0.9622
V_4	1.0222	0.9897	0.9894	1.0448	1.0531	1.0353	0.9984
V_5	0.9946	0.9951	0.9949	0.9941	0.9942	0.9961	0.9947
V_6	1.0205	1.0097	1.0092	1.0354	1.0239	1.0414	0.9920
V_7	1.1000	1.0999	1.1000	1.1000	1.1000	1.1000	1.1000
V_8	1.0727	1.0874	1.0876	1.0694	1.0500	1.0876	1.0588
V_9	1.0640	1.0981	1.0970	1.0560	1.0115	1.0990	1.0319
$T_{1\text{-}4}$	0.8725	1.1145	0.9654	0.8507	0.8589	1.0587	0.9507
$T_{2\text{-}7}$	0.8500	0.9560	0.9506	0.8501	0.8668	0.9700	0.8765
$T_{3\text{-}9}$	0.8500	0.9602	0.9439	0.9436	0.9597	0.9607	0.9471
p_{dr}	1.1267	1.0937	1.1101	1.1492	1.1442	1.0449	1.1057
p_{di}	1.1262	1.0932	1.1096	1.1486	1.1437	1.0444	1.1052
q_{dr}	0.2327	0.2229	0.2336	0.2396	0.2637	0.2199	0.2268
q_{di}	0.2777	0.2684	0.2726	0.2848	0.2835	0.2530	0.2728
i_d	0.7512	0.7329	0.7401	0.7671	0.7646	0.6968	0.7402
t_r	1.1094	1.1395	1.1472	1.0846	1.0799	1.0961	1.1310
t_i	1.1495	1.1430	1.1490	1.1491	1.1478	1.1465	1.1448
α (^{o})	7.3701	7.2390	7.7845	7.4122	9.2263	8.0815	7.3027
γ (^{o})	10.0007	10.0083	10.0001	10.0000	10.0054	10.0023	10.0668
v_{dr}	1.4999	1.4924	1.5000	1.4981	1.4966	1.4997	1.4938
v_{di}	1.4991	1.4916	1.4993	1.4973	1.4958	1.4990	1.4931
VD	0.2848	0.3103	0.3094	0.3115	0.2442	0.3671	0.2056
L_index	**0.1910**	0.19117	0.19131	0.1916	0.19165	0.19185	0.19172
Ploss (MW)	6.6243	8.1430	7.6935	4.3838	5.9291	7.5467	7.1576
Fuel Cost ($/h)	1360.2354	1365.2111	1352.3631	1297.3131	1338.4121	1365.7496	1356.9748

values was defined as follows:

$$init_pop_{[N\times d]} = \begin{bmatrix} x_{11} & x_{12} & x_{13} & \cdots & x_{1d} \\ x_{21} & x_{22} & x_{23} & \cdots & x_{2d} \\ x_{31} & x_{32} & x_{33} & \cdots & x_{3d} \\ \vdots & \vdots & \vdots & \vdots & \vdots \\ x_{N1} & x_{N2} & x_{N3} & \cdots & x_{Nd} \end{bmatrix}_{N\times d} \quad (33)$$

The proposed MSA-AC method for the OPF problem with two-terminal HVDC systems can be summarized as follows:

Step 1: First, the parameters of the power system such as fuel coefficients of the generator units, line data, bus data and power flow parameters are established. The total number of iterations (T), size of the population (N) and number of problem dimensions (d) are then determined. The initial population is produced within the limit values of the control variables such as the active power generation, generator bus voltage, transformer tap ratio, active power of the rectifier side, active power of the inverter side, reactive power of the rectifier side, reactive power of the inverter side and direct current.

Step 2: In order to determine the fitness values of the control variables in the initial population, the Newton Raphson-based power flow method is applied to the control variables. The Newton Raphson-based power flow method is run to check whether or not the specified inequality limitations and the dependent variables are within the limits. According to Equations (29) and (30), if any one of them violates the limits, the penalty function is used as in that of Equation (31).

Step 3: The group of each moth is described depending on its fitness.

Step 4: The new pathfinders, prospectors and onlookers are generated according to equations (2)-(11).

Step 5: Based on the power flow, the Newton Raphson method is applied to define the dependent variables of this problem and investigate the fitness value of the new pathfinders, prospectors and onlookers of the population.

Step 6: Based on the power flow, the Newton Raphson method is run to check whether or not the specified inequality limitations and the dependent variables are within the limits. According to Equations (29) and (30), if any one of them violates the limits, the penalty function is used as in Equation (31).

Step 7: Step 3 is repeated until the stopping criteria are met.

5) TEST SYSTEM 1

The modified WSCC 9-bus test system including three generators, three transformers, nine busses and a total of 315W and 115MVAR active and reactive loads is shown in Figure 8 [21], [37]. It can be seen that the two-terminal HVDC link is located between four and five busses instead of the AC transmission line.

Comparisons of the results of the other algorithms in the literature with the results of the proposed approach for the minimization of the total fuel cost are given in Table 9.

TABLE 12. Comparative results by the proposed MSA-AC and the other methods (for the fuel cost of the test system II).

Variable	MSA-AC	MSA	TLBO	FA	SSA	DA	MVO	BSA[21]	ABC[32]
P_{G1}	2.5051668	2.5559544	2.3991651	2.5087481	2.5143773	2.5111118	2.5538433	2.35847	3.49000
P_{G2}	5.8706402	5.8589102	5.8249131	5.8370734	5.81744	5.7997991	5.9012717	5.30634	5.97331
P_{G3}	6.5837861	6.6102955	6.598603	6.5699626	6.5730913	6.5734432	6.5914037	6.75987	7.00000
P_{G4}	6.2905354	6.3529881	6.4603749	6.4715412	6.4761024	6.4883692	6.3320169	6.62081	5.45566
P_{G5}	5.2099618	5.2212541	5.1999484	5.2167618	5.2075918	5.2153659	5.1339945	5.06120	5.47801
P_{G6}	6.6452831	6.588101	6.6521181	6.6798663	6.6416415	6.6934041	6.6353198	6.70167	4.00000
P_{G7}	5.7580268	5.723611	5.7039339	5.5948175	5.7164647	5.7072751	5.7427698	5.88666	5.34792
P_{G8}	5.6113796	5.5017234	5.5034046	5.4458441	5.4507155	5.4649964	5.4647382	5.63718	6.50000
P_{G9}	8.4091407	8.4667548	8.5237491	8.5340477	8.49768	8.4602633	8.49227	8.39473	8.74932
P_{G10}	10.083107	10.094384	10.127145	10.133347	10.103456	10.089241	10.145875	10.30272	11.00000
Q_{G1}	0.5365143	0.008921157	0.7782053	0.799215	-0.3389393	-1.545812	-0.2352696	-1.47115	-2.04424
Q_{G2}	4.291537	2.733248	5.061234	4.688015	6.34853	5.77245	3.272873	4.48391	3.75206
Q_{G3}	2.414283	2.945602	2.453983	2.348968	1.012603	2.322896	3.091853	0.57159	1.42014
Q_{G4}	1.191575	1.28316	1.988108	1.037109	1.183378	1.403414	0.7071777	2.11010	-0.13930
Q_{G5}	1.293733	1.469855	-0.6726621	1.415788	1.150692	1.253158	1.605302	-1.02441	0.52513
Q_{G6}	0.6530123	1.216831	-0.8897249	2.974896	3.52925	3.219085	2.174306	-1.43144	-0.30549
Q_{G7}	2.057811	1.130266	2.648149	1.195248	0.8149721	0.8351715	1.690169	2.64157	1.00298
Q_{G8}	0.5047549	0.6315904	0.6528367	0.7105009	-1.162921	0.2441377	-0.4393082	-1.47291	-0.24810
Q_{G9}	0.04584623	0.03420441	0.3875201	-0.7314853	1.226031	0.8539289	0.9771826	-1.04856	-0.81278
Q_{G10}	-0.5835927	0.8633345	0.1360738	-0.7389717	0.3172351	-0.6287286	0.4600586	-1.59251	-2.10976
V_1	1.0563	1.0888	1.0795	1.0128	1.0234	0.9982	1.0338	1.0643	1.027
V_2	1.0801	1.0831	1.0840	1.0436	1.0210	1.0159	1.0359	1.0409	1.023
V_3	1.0718	1.0714	1.0673	1.0384	1.0292	1.0294	1.0355	1.0460	1.029
V_4	1.0529	1.0493	1.0585	1.0225	1.0196	1.0257	1.0173	1.0417	1.022
V_5	1.0718	1.0650	1.0808	1.0415	1.0470	1.0522	1.0355	1.0647	1.041
V_6	1.0781	1.0696	1.0871	1.0482	1.0547	1.0606	1.0413	1.0700	1.046
V_7	1.0642	1.0598	1.0750	1.0327	1.0405	1.0436	1.0287	1.0611	1.035
V_8	1.0613	1.0589	1.0728	1.0291	1.0374	1.0392	1.0267	1.0602	1.034
V_9	1.0688	1.0972	1.0938	1.0281	1.0497	1.0287	1.0495	1.0914	1.051
V_{10}	1.0893	1.0862	1.0886	1.0590	1.0532	1.0712	1.0621	1.0624	1.051
V_{11}	1.0837	1.0762	1.0867	1.0541	1.0522	1.0660	1.0512	1.0647	1.048
V_{12}	1.0892	1.0962	1.0365	1.0985	1.0998	1.0311	1.0500	0.9863	1.066
V_{13}	1.0861	1.0856	1.0815	1.0556	1.0512	1.0682	1.0619	1.0581	1.048
V_{14}	1.0799	1.0773	1.0674	1.0515	1.0490	1.0633	1.0568	1.0524	1.044
V_{15}	1.0723	1.0690	1.0395	1.0471	1.0487	1.0560	1.0511	1.0364	1.028
V_{16}	1.0826	1.0790	1.0416	1.0592	1.0626	1.0668	1.0625	1.0411	1.033
V_{17}	1.0818	1.0795	1.0549	1.0505	1.0542	1.0559	1.0569	1.0520	1.042
V_{18}	1.0767	1.0752	1.0583	1.0446	1.0433	1.0444	1.0474	1.0493	1.037
V_{19}	1.0984	1.0969	1.0326	1.0737	1.0755	1.0834	1.0731	1.0291	1.014
V_{20}	1.0500	1.0053	1.0066	1.0758	0.9721	1.0211	1.0443	1.0701	1.044
V_{21}	1.0783	1.0736	1.0266	1.0666	1.0725	1.0744	1.0672	1.0269	1.026
V_{22}	1.0907	1.0849	1.0296	1.0913	1.0996	1.0992	1.0891	1.0273	1.030
V_{23}	1.0944	1.0834	1.0416	1.0847	1.0902	1.0908	1.0868	1.0409	1.032
V_{24}	1.0879	1.0833	1.0451	1.0666	1.0702	1.0739	1.0697	1.0457	1.039
V_{25}	1.0973	1.0999	1.1000	1.0585	1.0310	1.0379	1.0509	1.0532	1.047
V_{26}	1.0994	1.0991	1.0914	1.0444	1.0679	1.0629	1.0751	1.0892	1.083
V_{27}	1.0860	1.0848	1.0692	1.0415	1.0560	1.0541	1.0612	1.0690	1.061
V_{28}	1.0992	1.0984	1.0981	1.0183	1.0924	1.0739	1.0933	1.0956	1.094
V_{29}	1.0988	1.0978	1.0999	1.0114	1.0999	1.0775	1.0988	1.0889	1.089
V_{30}	1.0402	1.0098	1.0196	0.9945	0.9306	1.0999	0.9427	1.0744	1.060
V_{31}	1.0885	1.0923	1.0942	1.0545	1.0967	1.0989	1.0234	1.0857	1.069
V_{32}	1.0888	1.0635	1.0974	1.0007	0.9846	1.0250	1.0261	1.0731	1.068
V_{33}	1.0917	1.0618	1.0443	1.0999	1.1000	1.0357	1.0641	1.0703	1.071
V_{34}	1.0958	0.9842	1.1000	1.0641	1.0999	1.0511	0.9940	1.0056	1.098
V_{35}	1.0967	1.0506	1.0999	1.0291	1.0444	1.0393	1.0586	1.0706	1.100
V_{36}	1.0565	1.0929	1.1000	1.0180	1.0996	1.0987	1.0402	1.0493	1.040
V_{37}	1.0485	1.0139	1.1000	1.1000	0.9003	1.1000	1.0164	1.0014	1.065
V_{38}	1.0966	1.0987	1.0987	1.1000	1.1000	0.9929	1.0705	1.0500	1.100
V_{39}	1.0375	1.0869	1.0717	0.9912	1.0217	0.9852	1.0289	1.0546	1.006
$T_{2\text{-}30}$	1.0468	1.0717	1.0768	1.0638	1.0879	0.9021	1.0922	0.9463	0.933162
$T_{6\text{-}31}$	1.0782	1.0293	1.1000	1.0986	1.0965	1.0852	1.0902	1.0799	1.055100
$T_{10\text{-}32}$	1.0360	1.0693	1.0275	1.1000	1.0822	1.0842	1.0900	0.9931	1.001239
$T_{12\text{-}11}$	1.0300	1.0845	0.9719	1.0592	1.0681	0.9891	1.0550	0.9333	1.038348
$T_{12\text{-}13}$	1.0121	0.9871	0.9725	1.0608	1.0611	0.9773	0.9741	0.9586	1.032158
$T_{19\text{-}20}$	1.0427	1.0880	0.9959	0.9960	1.0999	1.0562	1.0269	0.9321	0.958201
$T_{19\text{-}33}$	1.0216	1.0508	1.0158	0.9891	0.9923	1.0665	1.0183	0.9881	0.945680
$T_{20\text{-}34}$	0.9780	1.0503	0.9068	1.0351	0.9000	0.9923	1.0826	1.0456	0.959304
$T_{22\text{-}35}$	0.9992	1.0452	0.9235	1.1000	1.0994	1.1000	1.0541	0.9396	0.932124
$T_{23\text{-}36}$	1.0819	1.0111	1.0002	1.0906	1.0039	1.0057	1.0820	1.0519	1.011136
$T_{25\text{-}37}$	1.0535	1.0955	1.0097	0.9728	1.0999	0.9453	1.0194	1.0122	0.972303
$T_{29\text{-}38}$	1.0022	0.9993	1.0056	0.9105	1.0156	1.0976	1.0394	1.0209	0.979414
p_{dr}	0.9848	1.2578	1.2386	1.3736	1.3818	1.3861	0.9655	1.1432	0.710262
p_{di}	0.9842	1.2569	1.2376	1.3727	1.3809	1.3851	0.9651	1.1423	0.709894
q_{dr}	0.4940	0.6426	0.2974	0.3687	0.3649	0.3244	0.4477	0.2889	0.178700
q_{di}	0.5449	0.4488	0.3559	0.3605	0.7176	0.3763	0.3518	0.3391	0.233957
i_d	0.7374	0.9533	1.0000	0.9344	0.9832	0.9968	0.6512	0.9491	0.607147
t_r	1.0244	1.0183	0.8837	1.0719	1.0261	0.9946	1.1452	0.8742	0.855936
t_i	1.0729	0.9879	0.9008	1.1000	1.1495	1.0394	1.1483	0.8924	0.891964
α (°)	24.9970	24.9325	7.1484	11.0833	10.2710	7.5385	23.4650	8.5608	7.3254
γ (°)	27.2940	16.0131	10.5065	10.0100	25.1680	10.0026	17.9528	11.4054	13.0568
v_{dr}	1.3354	1.3193	1.2386	1.4700	1.4054	1.3905	1.4828	1.2046	-
v_{di}	1.3346	1.3184	1.2376	1.4690	1.4045	1.3895	1.4821	1.2036	-
VD	2.3271	2.2747	1.8943	1.4498	1.6200	1.5689	1.6134	-	-
L_index	0.1902	0.1880	0.1856	0.1999	0.2033	0.1934	0.2070	-	-
Ploss (MW)	42.4184	43.0768	45.0055	44.8837	45.5294	45.9975	45.0779	-	-
Fuel Cost ($/h)	**63466.3658**	63476.4858	63498.8916	63501.7971	63508.7177	63516.0894	63514.2392	63598.8	64730.3

TABLE 13. Comparative results by the proposed MSA-AC and the other methods (for the VD of the test system II).

Variable	MSA-AC	MSA	TLBO	FA	SSA	DA	MVO
P_{G1}	3.4999993	1.4882506	3.0100611	3.3371867	3.1718952	1.0163569	2.9487168
P_{G2}	6.4835776	6.4742719	6.4853625	6.4998982	6.0299327	6.4762442	6.4797212
P_{G3}	4.7146491	4.8540732	5.3359922	6.3055609	6.9372561	7.2971987	5.1503824
P_{G4}	5.8059846	5.5901883	6.281367	6.4972749	4.7297761	4.4750017	7.3746302
P_{G5}	5.683012	5.3612238	5.1933439	5.7786839	4.140538	5.1244592	3.2575797
P_{G6}	4.6999871	7.4955047	4.0790817	7.2869312	7.2740691	5.8524032	7.4919026
P_{G7}	5.973038	6.1614936	7.4530733	3.2210749	5.3156821	6.0852081	3.7257303
P_{G8}	5.6006902	5.8023114	4.2399994	6.057333	5.2831157	6.9943683	6.0853486
P_{G9}	8.7429968	8.0232883	8.9865931	6.076893	8.2569751	7.9894118	8.6170191
P_{G10}	11.937529	11.9097	12.000000	11.994719	11.908516	11.726348	11.987484
Q_{G1}	6.068264	4.894706	3.727694	4.281895	4.979839	1.862385	5.581028
Q_{G2}	7.31646	7.379657	7.334901	7.262146	5.563758	7.870865	5.699702
Q_{G3}	-0.1284189	-0.1639275	0.1462036	0.5577383	1.240087	0.5478894	1.02797
Q_{G4}	4.666328	-2.650761	4.017106	-3.015858	4.17576	-0.2495928	-0.2679827
Q_{G5}	-1.819497	6.029696	-0.2428175	7.699124	-1.214804	2.675902	3.104177
Q_{G6}	3.493618	4.865338	0.8330093	1.794213	2.014899	3.762091	2.207855
Q_{G7}	-0.4310254	-0.57353	2.094422	0.41.6375	0.7055905	-0.5977763	0.2672734
Q_{G8}	-3.199469	-2.911022	-2.267336	-2.275238	-2.660002	-0.5322778	-2.757057
Q_{G9}	0.5717186	0.3410109	0.6415702	-0.250511	0.4084473	0.04552755	0.4971375
Q_{G10}	-0.2276408	-0.03991071	0.002236413	-0.07128568	-0.07592743	0.3029885	-0.08474675
V_1	0.9998	1.0000	1.0000	1.0000	0.9994	0.9997	0.9998
V_2	1.0216	1.0147	1.0136	1.0161	1.0179	1.0032	1.0176
V_3	1.0028	1.0002	0.9995	1.0000	1.0002	0.9947	1.0001
V_4	0.9868	0.9864	0.9846	0.9840	0.9823	0.9838	0.9848
V_5	1.0070	1.0070	1.0062	1.0057	1.0014	1.0070	1.0047
V_6	1.0135	1.0136	1.0129	1.0125	1.0078	1.0141	1.0111
V_7	0.9992	0.9995	0.9988	0.9983	0.9938	1.0002	0.9971
V_8	0.9964	0.9968	0.9961	0.9956	0.9913	0.9976	0.9944
V_9	1.0094	1.0121	1.0122	1.0110	1.0081	1.0163	1.0100
V_{10}	1.0000	1.0000	1.0021	1.0008	1.0038	1.0015	1.0058
V_{11}	1.0001	1.0002	1.0000	1.0006	1.0035	0.9999	1.0072
V_{12}	1.0000	1.0000	1.0000	1.0000	0.9999	1.0000	0.9999
V_{13}	1.0005	1.0003	1.0040	1.0000	1.0000	1.0028	1.0004
V_{14}	0.9943	0.9944	0.9979	0.9927	0.9941	0.9959	0.9943
V_{15}	0.9858	0.9862	0.9887	0.9851	0.9857	0.9869	0.9844
V_{16}	0.9974	0.9979	1.0000	0.9970	0.9973	0.9982	0.9954
V_{17}	0.9979	0.9976	0.9987	0.9975	0.9975	0.9973	0.9960
V_{18}	0.9984	0.9970	0.9976	0.9971	0.9971	0.9949	0.9962
V_{19}	1.0099	1.0149	1.0324	1.0211	1.0193	1.0130	1.0108
V_{20}	0.9999	1.0000	1.0000	1.0000	1.0000	1.0000	1.0006
V_{21}	0.9990	1.0000	0.9915	0.9920	0.9916	0.9992	0.9923
V_{22}	1.0184	1.0231	1.0011	1.0050	1.0058	1.0191	1.0080
V_{23}	0.9999	1.0000	1.0000	1.0000	1.0002	1.0001	1.0006
V_{24}	1.0017	1.0014	1.0036	1.0016	1.0012	1.0021	1.0001
V_{25}	1.0001	1.0000	1.0001	1.0000	1.0000	1.0108	1.0000
V_{26}	1.0014	1.0031	1.0020	1.0039	1.0024	1.0061	1.0012
V_{27}	0.9930	0.9944	0.9940	0.9949	0.9936	0.9956	0.9921
V_{28}	0.9989	1.0000	0.9989	1.0010	0.9999	1.0005	0.9996
V_{29}	1.0000	1.0002	1.0001	1.0000	1.0006	0.9999	1.0009
V_{30}	1.0737	1.0650	0.9972	1.0998	1.0630	1.0222	1.1000
V_{31}	1.1000	1.0986	1.0997	1.0997	1.1000	1.0897	1.0871
V_{32}	0.9615	1.0100	0.9560	0.9122	1.0140	0.9534	0.9429
V_{33}	1.0605	1.0814	1.0023	0.9110	1.0233	1.0494	0.9971
V_{34}	1.0216	1.0349	0.9763	1.0698	0.9924	0.9812	1.0250
V_{35}	1.0499	1.0454	0.9799	1.0213	1.0353	1.0594	1.1000
V_{36}	0.9769	0.9195	0.9479	0.9583	1.0689	1.0755	1.0222
V_{37}	0.9914	1.0414	1.0599	1.0066	0.9653	1.0088	0.9000
V_{38}	1.0066	0.9875	1.0044	1.0988	1.0053	1.0880	1.0366
V_{39}	0.9822	0.9862	0.9868	0.9853	0.9834	0.9928	0.9844
$T_{2\text{-}30}$	1.0496	1.0332	1.0886	0.9857	1.0390	1.0139	1.0083
$T_{6\text{-}31}$	1.0714	1.0749	1.0716	1.0692	1.0243	1.1000	1.0443
$T_{10\text{-}32}$	1.0318	0.9826	1.0445	1.0991	1.0048	1.0495	1.0844
$T_{12\text{-}11}$	1.0779	1.0732	1.1000	1.0673	1.0210	1.0984	1.0007
$T_{12\text{-}13}$	0.9724	0.9755	0.9558	0.9796	1.0150	0.9578	1.0319
$T_{19\text{-}20}$	0.9631	1.0712	1.0063	1.0991	0.9818	1.0259	1.0308
$T_{19\text{-}33}$	1.0130	0.9101	1.0926	1.0651	1.0571	0.9634	1.0095
$T_{20\text{-}34}$	0.9491	1.0757	1.0196	1.0641	0.9867	1.0731	1.0324
$T_{22\text{-}35}$	1.0139	1.0395	1.0325	1.0036	0.9934	1.0074	0.9371
$T_{23\text{-}36}$	1.0001	1.0517	1.0999	1.0535	0.9461	0.9103	0.9828
$T_{25\text{-}37}$	0.9337	0.9004	0.9001	0.9392	0.9671	0.9818	1.0205
$T_{29\text{-}38}$	1.0000	1.0167	1.0031	0.9080	0.9999	0.9194	0.9712
p_{dr}	1.2627	0.8609	1.3252	1.1611	1.2067	1.2117	0.9571
p_{di}	1.2618	0.8604	1.3242	1.1601	1.2059	1.2110	0.9564
q_{dr}	0.3473	0.3840	0.3080	0.4659	0.2733	0.3316	0.2990
q_{di}	0.3469	0.2251	0.3981	0.4299	0.3247	0.3108	0.2610
i_d	0.9708	0.6703	0.9966	0.9930	0.9034	0.8414	0.8338
t_r	1.0046	1.0472	1.0130	0.9398	1.0201	1.1101	0.8956
t_i	1.0115	0.9960	1.0435	0.9375	1.0420	1.1183	0.8940
α (^{o})	10.7597	22.2807	7.0148	18.5581	7.2548	11.8209	13.5753
γ (^{o})	10.0065	10.9303	11.9945	16.1679	10.1717	10.0068	10.0149
v_{dr}	1.3007	1.2843	1.3297	1.1692	1.3357	1.4400	1.1479
v_{di}	1.2997	1.2836	1.3287	1.1683	1.3348	1.4392	1.1470
VD	**0.13956**	0.14063	0.1441	0.1450	0.14859	0.15328	0.1527
L_index	0.2094	0.2110	0.2123	0.2148	0.2078	0.2128	0.2139
Ploss (MW)	59.8266	61.7557	52.1581	51.2270	50.4640	49.3992	57.5520
Fuel Cost ($/h)	65110.0154	64795.1049	65342.6942	65451.9451	64576.3002	65074.8257	65412.1459

TABLE 14. Comparative results by the proposed MSA-AC and the other methods (for the *L*-Index of the test system II).

Variable	MSA-AC	MSA	TLBO	FA	SSA	DA	MVO
P_{G1}	3.4950954	2.4720591	3.1419415	2.2642496	2.5127861	3.4999597	3.4999871
P_{G2}	5.1708088	6.0277466	4.5207187	4.0173968	5.2318132	5.048605	4.5563847
P_{G3}	4.1997673	6.8092832	5.0690865	4.6691307	3.2410079	4.5658755	5.3268413
P_{G4}	6.0414455	7.4987617	7.1087179	7.3622293	6.3619508	6.7476937	5.8129435
P_{G5}	6.49804	4.8605397	5.3613687	5.3969155	6.4999778	4.9712445	5.9459009
P_{G6}	7.4890201	5.8309772	7.4587226	6.1856522	7.369078	6.324504	6.5478265
P_{G7}	5.6515206	5.3157254	5.30691	7.5000000	7.499861	6.9004017	7.4772159
P_{G8}	3.4406911	6.476352	5.4658619	5.9444142	4.6925415	3.9814604	5.2758092
P_{G9}	9.000000	5.628462	7.6682605	8.8850732	7.6253581	8.994515	6.556557
P_{G10}	11.998942	11.999828	11.968044	10.954577	11.977583	11.999606	11.998784
Q_{G1}	-1.522809	2.416128	5.548324	3.972401	2.129023	2.359535	0.3823306
Q_{G2}	2.016927	0.2445719	-0.3789393	1.522827	1.094903	3.612035	2.577559
Q_{G3}	3.017576	5.010798	4.757235	3.537214	3.515326	2.771844	2.882253
Q_{G4}	-1.489512	0.8457207	2.709167	5.106889	1.658837	-4.439372	-3.695139
Q_{G5}	4.561244	1.75338	0.005661496	-1.741943	1.071616	3.907779	7.470077
Q_{G6}	2.033243	2.656353	3.143169	4.057594	1.013707	5.982303	1.983524
Q_{G7}	0.9697402	-0.2941917	-0.3906121	-0.623602	2.86467	-0.6575916	1.492805
Q_{G8}	1.553629	-1.217267	-4.007395	-2.438405	-1.028565	-0.6363038	0.2121458
Q_{G9}	0.1393855	-0.5784958	0.08654347	0.3795801	-0.3896372	0.4002962	-0.6000748
Q_{G10}	0.5412613	0.5265131	0.6357492	0.1660514	0.2500266	-0.1009328	0.02658509
V_1	1.0882	1.0984	1.0996	1.0925	1.0953	1.0914	1.0882
V_2	1.0819	1.0988	1.1000	1.0999	1.0998	1.1000	1.0918
V_3	1.0743	1.0815	1.0805	1.0838	1.0833	1.0787	1.0819
V_4	1.0572	1.0545	1.0531	1.0642	1.0615	1.0658	1.0674
V_5	1.0748	1.0664	1.0639	1.0795	1.0750	1.0849	1.0851
V_6	1.0797	1.0702	1.0673	1.0841	1.0791	1.0904	1.0904
V_7	1.0693	1.0609	1.0585	1.0734	1.0691	1.0790	1.0790
V_8	1.0681	1.0603	1.0581	1.0720	1.0680	1.0771	1.0772
V_9	1.0999	1.0998	1.1000	1.1000	1.1000	1.1000	1.0999
V_{10}	1.0997	1.0978	1.0999	1.0996	1.1000	1.0999	1.0990
V_{11}	1.0913	1.0914	1.0900	1.0978	1.0947	1.0941	1.0999
V_{12}	0.9778	1.0908	1.0963	1.0413	1.0103	1.0834	1.0434
V_{13}	1.0963	1.0865	1.0923	1.0879	1.0915	1.0948	1.0871
V_{14}	1.0893	1.0808	1.0865	1.0829	1.0860	1.0807	1.0832
V_{15}	1.0773	1.0744	1.0752	1.0734	1.0752	1.0515	1.0751
V_{16}	1.0860	1.0851	1.0842	1.0834	1.0848	1.0531	1.0853
V_{17}	1.0844	1.0857	1.0840	1.0850	1.0855	1.0651	1.0858
V_{18}	1.0793	1.0830	1.0814	1.0831	1.0833	1.0689	1.0831
V_{19}	1.0998	1.0992	1.0996	1.0999	1.0999	0.9948	1.0984
V_{20}	1.0321	1.0931	1.0714	1.0575	1.0127	1.0167	1.0672
V_{21}	1.0843	1.0841	1.0825	1.0828	1.0808	1.0673	1.0831
V_{22}	1.1000	1.0987	1.0980	1.1000	1.0957	1.0998	1.0989
V_{23}	1.0959	1.0862	1.0841	1.0790	1.0997	1.0744	1.0948
V_{24}	1.0909	1.0891	1.0877	1.0860	1.0899	1.0596	1.0898
V_{25}	1.0999	1.0966	1.0780	1.0959	1.0998	1.1000	1.0997
V_{26}	1.0997	1.0995	1.0945	1.0998	1.0998	1.0942	1.1000
V_{27}	1.0874	1.0882	1.0844	1.0876	1.0882	1.0754	1.0884
V_{28}	1.0969	1.0956	1.0993	1.0999	1.0939	1.0983	1.0938
V_{29}	1.0961	1.0927	1.0999	1.0999	1.0912	1.0997	1.0905
V_{30}	1.1000	1.0983	1.0979	1.0998	1.0986	1.1000	1.0976
V_{31}	1.0999	1.0999	1.0999	1.1000	1.0997	1.1000	1.1000
V_{32}	1.1000	1.1000	1.0998	1.0998	1.0989	1.0996	1.0999
V_{33}	1.0695	1.0995	1.0644	1.0965	1.0883	0.9593	0.9783
V_{34}	1.0181	1.0355	1.0975	0.9269	1.0505	1.1000	1.0937
V_{35}	1.0630	1.0852	1.1000	1.0999	1.1000	1.1000	1.0370
V_{36}	1.0999	1.0388	1.0189	1.0281	1.0585	1.0338	1.1000
V_{37}	1.0938	1.1000	1.1000	1.0989	1.0250	0.9829	1.0373
V_{38}	1.0748	1.0421	1.0997	1.0064	1.0999	1.1000	1.0991
V_{39}	1.0850	1.0901	1.0921	1.0823	1.0852	1.0790	1.0789
$T_{2\text{-}30}$	0.9604	1.0373	1.014	1.0626	1.0333	1.0350	0.9991
$T_{6\text{-}31}$	1.0172	0.9696	0.9580	1.0130	0.9972	1.0636	1.0410
$T_{10\text{-}32}$	1.0494	1.0800	1.0810	1.0584	1.0612	1.0451	1.0447
$T_{12\text{-}11}$	0.9179	0.9578	0.9890	0.9042	0.9005	1.0282	0.9005
$T_{12\text{-}13}$	0.9000	1.0978	1.0589	1.0561	0.9865	0.9862	1.0669
$T_{19\text{-}20}$	1.1000	1.0074	1.0076	0.9967	1.0763	1.0076	1.0958
$T_{19\text{-}33}$	1.0105	1.0102	1.0698	1.0681	1.0321	0.9703	1.0649
$T_{20\text{-}34}$	1.1000	1.0885	0.9771	1.1000	0.9808	0.9824	1.1000
$T_{22\text{-}35}$	1.0572	1.0434	1.0324	1.0474	1.0043	1.0724	1.0841
$T_{23\text{-}36}$	1.0125	1.0313	1.0459	1.0181	1.0999	1.0103	1.0178
$T_{25\text{-}37}$	1.0363	0.9700	0.9079	0.9495	1.0465	1.1000	1.0612
$T_{29\text{-}38}$	1.0206	1.0408	1.0014	1.0967	0.9873	1.0041	0.9852
p_{dr}	1.4988	1.4953	1.2616	1.2390	1.0790	1.2196	1.1049
p_{di}	1.4978	1.4943	1.2609	1.2383	1.0785	1.2190	1.1044
q_{dr}	0.3369	0.4185	0.2659	0.2609	0.2609	0.2539	0.2223
q_{di}	0.3987	0.3999	0.3201	0.3138	0.2632	0.3067	0.2712
i_d	1.0000	0.9986	0.8419	0.8305	0.7193	0.8134	0.7369
t_r	1.0443	1.0653	1.0437	1.0425	1.0522	1.0494	1.0455
t_i	1.0856	1.0877	1.0864	1.0703	1.0765	1.0736	1.0705
α (^{o})	7.1969	11.6948	7.0598	7.1030	10.3335	7.0435	7.0015
γ (^{o})	10.0133	10.1291	10.0000	10.0082	10.0026	10.0023	10.0057
v_{dr}	1.4988	1.4974	1.4984	1.4919	1.5000	1.4995	1.4994
v_{di}	1.4978	1.4964	1.4976	1.4910	1.4992	1.4987	1.4986
VD	2.4021	2.4892	2.4502	2.4721	2.3939	2..2495	2.5073
L_index	**0.17696**	0.1775	0.17815	0.17924	0.17993	0.18244	0.18101
Ploss (MW)	44.2031	37.6437	52.6624	63.6649	46.9140	49.0904	45.5408
Fuel Cost ($/h)	65405.2294	64735.8671	64589.6365	64905.8409	65685.9532	64974.2911	65101.0205

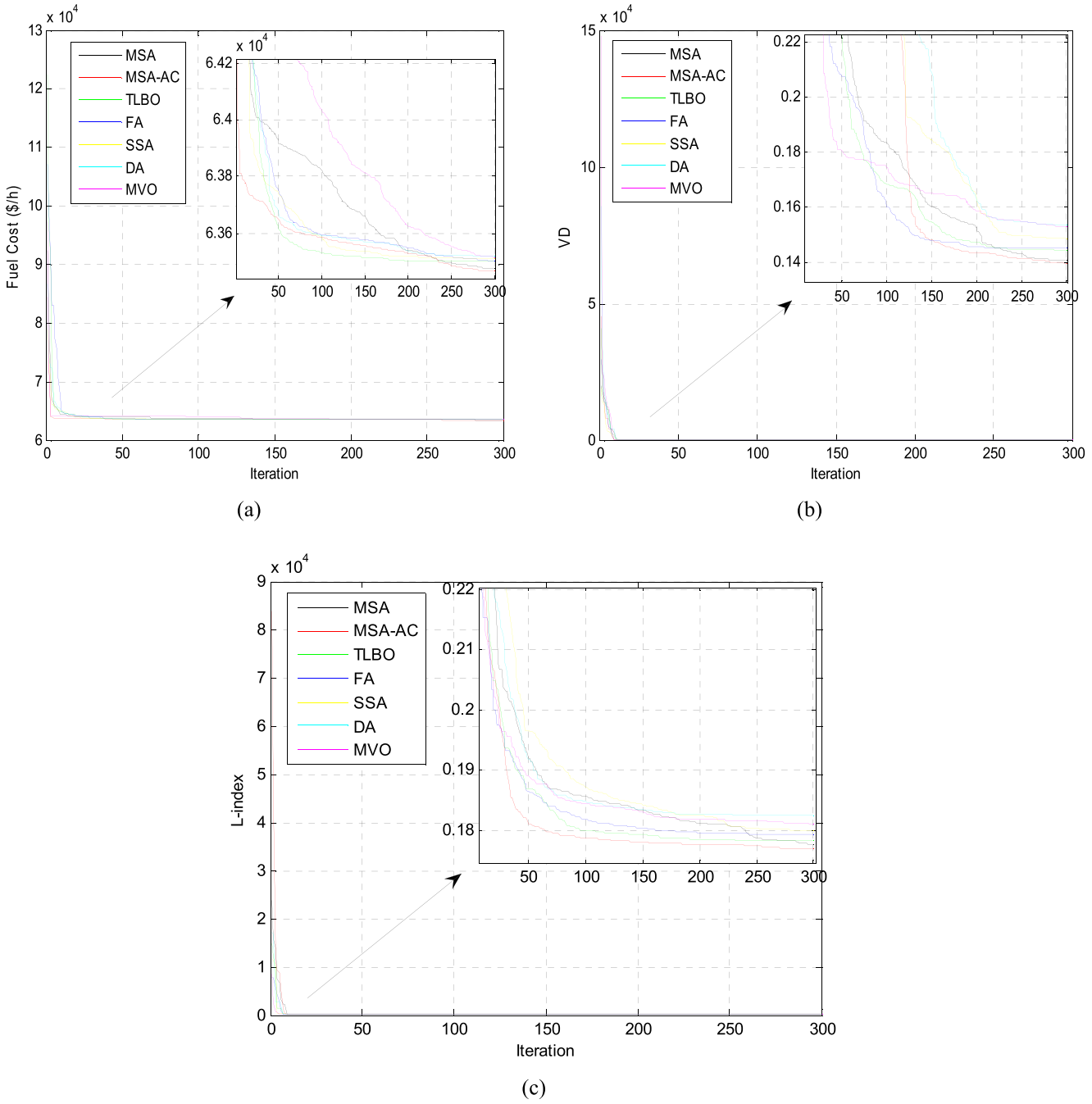

FIGURE 10. Comparative convergence curves of the MSA-AC and the other methods for test system 2.

It may be observed that the total minimum fuel cost from the proposed MSA-AC, MSA, TLBO, FA, SSA, DA, MVO, BSA [21] and GA [37] methods were 1132.8925 $/h, 1133.3953 $/h, 1133.719 $/h, 1134.2706 $/h, 1134.4888 $/h, 1136.5176 $/h, 1136.3679 $/h, 1135.032 $/h and 1145.9525 $/h, respectively. In other words, the proposed MSA-AC method exhibited the minimum fuel cost within the specified limits. The total fuel cost value of the proposed MSA-AC was 0.04436%, 0.0729%, 0.121496%, 0.140706%, 0.318965%, 0.305834%, 0.188496% and 1.139663% lower than those obtained from the MSA, TLBO, FA, SSA, DA, MVO, BSA and GA, respectively. The comparative convergence curves of the minimum fuel cost for the MSA-AC, the used optimization algorithms and the other methods in the literature are presented in Figure 9(a). From the figure it is obvious that the value of the total minimum fuel cost converges a fewer minimum value for the MSA-AC method than for the other optimization methods. The results of the second objective function the used as voltage deviation are presented in Table 10. In second objective function, the minimization

of the voltage deviation of the test system, the proposed MSA-AC gives best output of 0.13179, consequently better than the used other optimization algorithms. Figure 9(b) shows the convergence curves of the obtained voltage deviation values from the used optimization algorithms for the modified WSCC 9-bus test system.

In the third objective function, applying the OPF problem with two-terminal HVDC systems to the proposed MSA-AC importantly decrease the value of L-index according to the other methods. The simulation results of the MSA-AC technique are compared with the other heuristic techniques for the L-index indicator. The comparison results are shown in Table 11. From the Table 11 it is obvious that in MSA-AC approach, L-index is 0.1910, which is reduce 0.088926%, 0.16204%, 0.313152%, 0.3391599%, 0.4430544%, 0.375547% than in comparison with MSA, TLBO, FA, SSA, DA and MVO, respectively. The convergence curves of the L-index values of the proposed approach and the other optimization algorithms for the test system are shown in Figure 9(c). From the figure it is clear that the value of the L-index converges a faster to minimum value for the MSA-AC method than for the other optimization methods.

6) TEST SYSTEM 2

The modified New England 39-bus test system including a two-terminal HVDC link is located between 14 and 4 busses instead of the AC transmission line as in the original New England test system. The comparisons of the obtained results from the BSA [21], ABC [32], MSA and the proposed MSA-AC algorithms are given in Table 12. Table 12 shows that the total minimum fuel costs from the proposed MSA-AC, MSA, TLBO, FA, SSA, DA, MVO, BSA and ABC methods were 63466.3658 \$/h, 63476.4858 \$/h, 63498.8916 \$/h, 63501.7971 \$/h, 63508.7177 \$/h, 63516.0894 \$/h, 63514.2392 \$/h, 63598.8 \$/h, and 64730.3 \$/h, respectively.

From the Table 12 it is obvious that in MSA-AC approach, the total minimum fuel cost is 63466.3658 \$/h, which is reduce 0.01594%, 0.05122%, 0.05579%, 0.06668%, 0.07828%, 0.07537%, 0.20823%, 1.95261% than in comparison with MSA, TLBO, FA, SSA, DA and MVO, respectively. To put it another way, the proposed MSA-AC has 132.4342 \$/h less total fuel cost than the BSA method in the literature. Figure 10(a) depicts the comparative convergence curves of the minimum fuel cost for the MSA-AC, the used optimization algorithms and the other methods in the literature. From the figure, it can be seen that the value of the total minimum fuel cost converges a fewer minimum value for the MSA-AC method than for the other algorithms. In second objective function for the test system II, the obtained voltage deviation results from the optimization methods are expressed in Table 13. For minimization of the voltage deviation of the test system, the proposed MSA-AC gives best output of 0.13956. Consequently, this result is better than the other MSA, TLBO, FA, SSA, DA and MVO, respectively. Figure 10(b) shows the convergence curves of the obtained voltage deviation values from the used optimization algorithms for the modified New England 39-bus test system.

In the third objective function, the proposed MSA-AC and the other optimization algorithms are applied to solve OPF problem with two-terminal HVDC systems. The proposed MSA-AC importantly reduce the value of L-index according to the other algorithms. The simulation results of the proposed method are compared to the other optimization algorithms for the L-index indicator. The comparison results are shown in Table 14. From the Table 14 it can be seen that in proposed approach, L-index is 0.17696, which is decrease 0.30422%, 0.66797%, 1.272037%, 1.65064%, 3.00372%, 2.23744% than in comparison with MSA, TLBO, FA, SSA, DA and MVO, respectively. The convergence curves of the L-index values of the MSA-AC and the other algorithms for the test system II are shown in Figure 10(c). From the figure it is obvious that the value of the L-index converges a faster to minimum value for the MSA-AC method than for the other MSA, TLBO, FA, SSA, DA, MVO algorithms.

IV. CONCLUSION

In this paper, a proposed MSA method based on an arithmetic crossover operator (MSA-AC) was presented. The combination of the crossover operator based on population diversity with the arithmetic crossover operator offers a more rapid convergence to the optimal solution and a better quality solution in the search space than the traditional MSA and the other optimization algorithms. The proposed MSA-AC method was applied to solve two different types of optimization problems (in constrained optimization problem and in optimal power flow with two-terminal HVDC systems). First, the proposed MSA-AC approach was tested to evaluate its performance in benchmark test functions (23 standard benchmark and six composite benchmark test functions). The results of the simulation study showed that the proposed MSA-AC approach was more successful in the search for the best result compared to the other methods in the literature. Secondly, the proposed approach was used to solve the OPF problem with two-terminal HVDC systems under the different three objective functions (the modified New England 39-bus and the modified WSCC 9-bus test systems). These objective functions are depicted as the total fuel cost, improvement of the voltage deviation and enhancement of the voltage stability. The results of the proposed MSA-AC were compared to the results of other methods in the literature. According to these comparison results, the proposed approach was proven to increase the performance, robustness and efficiency of the MSA method. Additionally, the convergence velocity to the optimal solution and the success in finding the best solution as performed by the MSA were increased by means of the proposed MSA-AC method. Consequently, the proposed approach can be said to improve the balance of exploration and exploitation for the solution of optimization problems.

REFERENCES

[1] R. Storn and K. Price, "Differential evolution—A simple and efficient heuristic for global optimization over continuous spaces," *J. Global Optim.*, vol. 11, no. 4, pp. 341–359, 1997.
[2] Z. W. Geem, J. H. Kim, and G. V. Loganathan, "A new heuristic optimization algorithm: Harmony search," *J. Simul.*, vol. 76, no. 2, pp. 60–68, Feb. 2001.
[3] A. Hatamlou, "Black hole: A new heuristic optimization approach for data clustering," *Inf. Sci.*, vol. 222, pp. 175–184, Feb. 2012.
[4] A. Kaveh and M. Khayatazad, "A new meta-heuristic method: Ray Optimization," *Comput. Struct.*, vols. 112–113, pp. 283–294, Dec. 2012.
[5] D. E. Goldberg, *Genetic Algorithms in Search, Optimization and Machine Learning*. Reading, MA, USA: Addison-Wesley, 1989.
[6] O. K. Erol and I. Eksin, "A new optimization method: Big bang–big crunch," *Adv. Eng. Softw.*, vol. 37, no. 2, pp. 106–111, 2006.
[7] X.-S. Yang, "Firefly algorithm, stochastic test functions and design optimisation," *Int. J. Bio-Inspired Comput.*, vol. 2, no. 2, pp. 78–84, Mar. 2010.
[8] A. H. Gandomi and A. H. Alavi, "Krill herd: A new bio-inspired optimization algorithm," *Commun. Nonlinear Sci. Numer. Simul.*, vol. 17, pp. 4831–4845, May 2012.
[9] R. V. Rao, V. J. Savsani, and D. P. Vakharia, "Teaching–learning-based optimization: An optimization method for continuous non-linear large scale problems," *Inf. Sci.*, vol. 183, no. 1, pp. 1–15, Jan. 2012.
[10] B. Dogan and T. Olmez, "A new metaheuristic for numerical function optimization: Vortex search algorithm," *Inf. Sci.*, vol. 293, pp. 125–145, Feb. 2015.
[11] S. Mirjalili, A. H. Gandomi, S. Z. Mirjalili, S. Saremi, H. Faris, and S. M. Mirjalili, "Salp swarm algorithm: A bio-inspired optimizer for engineering design problems," *Adv. Eng. Softw.*, vol. 114, pp. 163–191, Dec. 2017.
[12] S. Mirjalili and A. Lewis, "The whale optimization algorithm," *Adv. Eng. Softw.*, vol. 95, pp. 51–67, May 2016.
[13] S. Mirjalili, "SCA: A sine cosine algorithm for solving optimization problems," *Knowl.-Based Syst.*, vol. 96, pp. 120–133, Mar. 2016.
[14] M. S. Kiran, "TSA: Tree-seed algorithm for continuous optimization," *Expert Syst. Appl.*, vol. 42, no. 19, pp. 6686–6698, Nov. 2015.
[15] S. Mirjalili, "Dragonfly algorithm: A new meta-heuristic optimization technique for solving single-objective, discrete, and multi-objective problems," *Neural Comput. Appl.*, vol. 27, no. 4, pp. 1053–1073, May 2016.
[16] S. Mirjalili, S. M. Mirjalili, and A. Lewis, "Grey wolf optimizer," *Adv. Eng. Softw.*, vol. 69, pp. 46–61, Mar. 2014.
[17] S. Mirjalili, S. M. Mirjalili, and A. Hatamlou, "Multi-verse optimizer: A nature-inspired algorithm for global optimization," *Neural Comput. Appl.*, vol. 27, no. 2, pp. 495–513, Feb. 2016.
[18] A.-A. A. Mohamed, Y. S. Mohamed, A. A. M. El-Gaafary, and A. M. Hemeida, "Optimal power flow using moth swarm algorithm," *Electr. Power Syst. Res.*, vol. 142, pp. 190–206, Jan. 2017.
[19] S. Saremi, S. Mirjalili, and A. Lewis, "Grasshopper optimisation algorithm: Theory and application," *Adv. Eng. Softw.*, vol. 105, pp. 30–47, Mar. 2017.
[20] A. E. Eiben and C. A. Schippers, "On evolutionary exploration and exploitation," *Fundam. Inform.*, vol. 35, nos. 1–4, pp. 35–50, Aug. 1998.
[21] K. Ayan and U. Kılıç, "Optimal power flow of two-terminal HVDC systems using backtracking search algorithm," *Int. J. Elect. Power Energy Syst.*, vol. 78, pp. 326–335, Jun. 2016.
[22] W. Bai, I. Eke, and K. Y. Lee, "An improved artificial bee colony optimization algorithm based on orthogonal learning for optimal power flow problem," *Control Eng. Pract.*, vol. 61, pp. 163–172, Apr. 2017.
[23] H. Pulluri, R. Naresh, and V. Sharma, "An enhanced self-adaptive differential evolution based solution methodology for multiobjective optimal power flow," *Appl. Soft Comput.*, vol. 54, pp. 229–245, May 2017.
[24] A. Mukherjee, P. K. Roy, and V. Mukherjee, "Transient stability constrained optimal power flow using oppositional krill herd algorithm," *Int. J. Elect. Power Energy Syst.*, vol. 83, pp. 283–297, Dec. 2016.
[25] H. R. E. H. Bouchekara, A. E. Chaib, M. A. Abido, and R. A. El-Sehiemy, "Optimal power flow using an improved colliding bodies optimization algorithm," *Appl. Soft Comput.*, vol. 42, pp. 119–131, May 2016.
[26] S. S. Reddy and C. S. Rathnam, "Optimal power flow using glowworm swarm optimization," *Int. J. Elect. Power Energy Syst.*, vol. 80, pp. 128–139, Sep. 2016.
[27] Y. Tan *et al.*, "Improved group search optimization method for optimal power flow problem considering valve-point loading effects," *Neurocomputing*, vol. 148, pp. 229–239, Jan. 2015.
[28] R. Roy and H. T. Jadhav, "Optimal power flow solution of power system incorporating stochastic wind power using Gbest guided artificial bee colony algorithm," *Int. J. Elect. Power Energy Syst.*, vol. 64, pp. 562–578, Jan. 2015.
[29] H. R. E. H. Bouchekara, "Optimal power flow using black-hole-based optimization approach," *Appl. Soft Comput.*, vol. 24, pp. 879–888, Nov. 2014.
[30] M. Ghasemi, S. Ghavidel, E. Akbari, and A. A. Vahed, "Solving nonlinear, non-smooth and non-convex optimal power flow problems using chaotic invasive weed optimization algorithms based on chaos," *Energy*, vol. 73, pp. 340–353, Aug. 2014.
[31] U. Kılıç, K. Ayan, and U. Arifoğlu, "Optimizing reactive power flow of HVDC systems using genetic algorithm," *Int. J. Elect. Power Energy Syst.*, vol. 55, pp. 1–12, Feb. 2014.
[32] U. Kılıç and K. Ayan, "Optimizing power flow of AC–DC power systems using artificial bee colony algorithm," *Int. J. Elect. Power Energy Syst.*, vol. 53, pp. 592–602, Dec. 2013.
[33] U. Kılıç and K. Ayan, "Artificial bee colony algorithm based optimal reactive power flow of two-terminal HVDC systems," *Turkish J. Elect. Eng. Comput. Sci.*, vol. 24, no. 3, pp. 1075–1090, 2016.
[34] F. Yalçn and U. Arifoğlu, "Optimal reactive power flow solution in multiterminal AC-DC systems based on artificial bee colony algorithm," *Turkish J. Elect. Eng. Comput. Sci.*, vol. 22, no. 5, pp. 1159–1176, 2014.
[35] B. S. Babu and S. Palaniswami, "Teaching learning based algorithm for OPF with DC link placement problem," *Int. J. Elect. Power Energy Syst.*, vol. 73, pp. 773–781, Dec. 2015.
[36] F. Yalçn and U. Arifoğlu, "A new approach based on genetic algorithm for optimal reactive power flow solution in multi-terminal AC-DC systems," *Przegląd Elektrotechniczny*, vol. 89, no. 3a, pp. 231–235, 2013.
[37] U. Kılıç and K. Ayan, "Optimal power flow solution of two-terminal HVDC systems using genetic algorithm," *Elect. Eng.*, vol. 96, no. 1, pp. 65–77, Mar. 2014.
[38] Q. Niu, H. Zhang, X. Wang, K. Li, and G. W. Irwin, "A hybrid harmony search with arithmetic crossover operation for economic dispatch," *Int. J. Elect. Power Energy Syst.*, vol. 62, pp. 237–257, Nov. 2014.
[39] X. Yao, Y. Liu, and G. Lin, "Evolutionary programming made faster," *IEEE Trans. Evol. Comput.*, vol. 3, no. 2, pp. 82–102, Jul. 1999.
[40] J. J. Liang, P. N. Suganthan, and K. Deb, "Novel composition test functions for numerical global optimization," in *Proc. IEEE Swarm Intell. Symp. (SIS)*, Jun. 2005, pp. 68–75.
[41] P. N. Suganthan *et al.*, "Problem definitions and evaluation criteria for the CEC 2005 special session on real-parameter optimization," Nanyang Technol. Univ., Singapore, Tech. Rep., 2005.
[42] R. D. Zimmerman, C. E. Murillo-Sánchez, and R. J. Thomas, "MATPOWER: Steady-state operations, planning, and analysis tools for power systems research and education," *IEEE Trans. Power Syst.*, vol. 26, no. 1, pp. 12–19, Feb. 2011.
[43] *MATPOWER*. [Online]. Available: http://www.pserc.cornell.edu/matpower/

SERHAT DUMAN was born in Bandirma, Turkey, in 1981. He received the B.S. degree in electrical education from Abant Izzet Baysal University, Bolu, Turkey, in 2008, the M.S. degree from the Department of Electrical Education, Duzce University, Turkey, in 2010, and the Ph.D. degree from the Department of Electrical Engineering, Kocaeli University, Turkey, in 2015. He is currently an Assistant Professor with the Department of Electrical and Electronics Engineering, Technology Faculty, Duzce University. His areas of research include power system planning, operation and economics, optimization techniques, renewable energy resources, and artificial intelligence applications.